NAVAL POSTGRADUATE SCHOOL
Monterey, California

THESIS

AMBIENT NOISE CHARACTERISTICS DURING THE SHEBA EXPERIMENT

by

Ronald R. Shaw Jr.

March 2000

Thesis Advisor:	Robert H. Bourke
Second Readers:	Peter S. Guest
	James H. Wilson

Approved for public release; distribution is unlimited.

REPORT DOCUMENTATION PAGE

Form Approved
OMB No. 0704-0188

1. AGENCY USE ONLY *(Leave blank)*	2. REPORT DATE	3. REPORT TYPE AND DATES COVERED
	March 2000	Master's Thesis

4. TITLE AND SUBTITLE
Ambient Noise Characteristics during the SHEBA experiment

5. FUNDING NUMBERS

6. AUTHOR(S)
Shaw, Ronald R.

7. PERFORMING ORGANIZATION NAME(S) AND ADDRESS(ES)
Naval Postgraduate School
Monterey, CA 93943-5000

8. PERFORMING ORGANIZATION REPORT NUMBER

SPONSORING / MONITORING AGENCY NAME(S) AND ADDRESS(ES)
Office of Naval Research
High Latitude Dynamics Program (322HL)
800 N. Quincy St.
Arlington, VA 22217

9. SPONSORING / MONITORING AGENCY REPORT NUMBER
N0001499WR30182
N0001400WR20281

11. SUPPLEMENTARY NOTES
The views expressed in this thesis are those of the author and do not reflect the official policy or position of the Department of Defense or the U.S. Government.

12a. DISTRIBUTION / AVAILABILITY STATEMENT
Approved for public release; distribution unlimited.

12b. DISTRIBUTION CODE

13. ABSTRACT *(maximum 200 words)*
The ambient noise data recorded by two free-drifting buoys during the 1997-98 SHEBA experiment presented a unique opportunity to gauge the noise field of the Arctic Ocean in a unique and changing environment. The two buoys drifted in unison for 12 months, providing an hourly ambient noise data set between 50 and 1000 Hz. The drift pattern was divided into five legs in response to the season or major changes in the direction of ice flow. The two buoys exhibited similar median spectra for all frequencies. When examined on a seasonal basis, summer low frequency (< 200 Hz) noise levels were much closer to winter noise levels than past studies. This was mainly due to the low number of storms during the winter of 1997-98, which resulted in lower winter median noise levels. When compared with previous ambient noise studies in the Beaufort Sea, the SHEBA noise data were consistent with the concept that noise levels decrease (especially in summer) during the years when cyclonic atmospheric circulation dominates the west Arctic. Cross correlation analysis indicated a strong association of wind speed and wind stress to ambient noise. Locally measured wind stress (as opposed to that computed using the geostrophic wind) did not substantially improve the correlation with ambient noise. Two tools to conceptualize the Arctic noise field were employed during the SHEBA experiment: the use of RADARSAT with RGPS and the PIPS computation of energy dissipation rate. By comparing the output from these two systems with the ambient noise record, their effectiveness and usefulness as input to an Arctic ambient noise model could be determined. Several notable events in the winter and summer noise record were examined utilizing RGPS and PIPS. The event analysis confirmed the fact that distant noise sources can have an effect on a local noise field. RGPS and PIPS were not useful in the summer due to the open nature of the icepack.

14. SUBJECT TERMS
Oceanography, Ambient Noise, Arctic, PIPS, RGPS, SHEBA

15. NUMBER OF PAGES
119

16. PRICE CODE

17. SECURITY CLASSIFICATION OF REPORT	18. SECURITY CLASSIFICATION OF THIS PAGE	19. SECURITY CLASSIFI- CATION OF ABSTRACT	20. LIMITATION OF ABSTRACT
Unclassified	Unclassified	Unclassified	UL

NSN 7540-01-280-5500

Standard Form 298 (Rev. 2-89)
Prescribed by ANSI Std. 239-18

Approved for public release; distribution is unlimited

AMBIENT NOISE CHARACTERISTICS DURING THE SHEBA EXPERIMENT

Ronald R. Shaw Jr.
Lieutenant, United States Navy
B.S., United States Naval Academy, 1992

Submitted in partial fulfillment of the
requirements for the degree of

MASTER OF SCIENCE IN METEOROLOGY AND PHYSICAL OCEANOGRAPHY

from the

NAVAL POSTGRADUATE SCHOOL
March 2000

Author: Ronald R Shaw Jr
Ronald R. Shaw Jr.

Approved by: Robert H. Bourke
Robert H. Bourke, Thesis Advisor

Pete S. Guest
Peter S. Guest, Second Reader

James H. Wilson
James H. Wilson, Second Reader

Roland W. Garwood Jr., Chairman, Department of Oceanography

ABSTRACT

The ambient noise data recorded by two free-drifting buoys during the 1997-98 SHEBA experiment presented a unique opportunity to gauge the noise field of the Arctic Ocean in a unique and changing environment. The two buoys drifted in unison for 12 months, providing an hourly ambient noise data set between 50 and 1000 Hz. The drift pattern was divided into five legs in response to the season or major changes in the direction of ice flow.

The two buoys exhibited similar median spectra for all frequencies. When examined on a seasonal basis, summer low frequency (< 200 Hz) noise levels were much closer to winter noise levels than past studies. This was mainly due to the low number of storms during the winter of 1997-98, which resulted in lower winter median noise levels.

When compared with previous ambient noise studies in the Beaufort Sea, the SHEBA noise data were consistent with the concept that noise levels decrease (especially in summer) during the years when cyclonic atmospheric circulation dominates the west Arctic.

Cross correlation analysis indicated a strong association of wind speed and wind stress to ambient noise. Locally measured wind stress (as opposed to that computed using the geostrophic wind) did not substantially improve the correlation with ambient noise.

Two tools to conceptualize the Arctic noise field were employed during the SHEBA experiment: the use of RADARSAT with RGPS and the PIPS computation of energy dissipation rate. By comparing the output from these two systems with the ambient noise record, their effectiveness and usefulness as input to an Arctic ambient noise model could be determined. Several notable events in the winter and summer noise

record were examined utilizing RGPS and PIPS. The event analysis confirmed the fact that distant noise sources can have an effect on a local noise field. RGPS and PIPS were not useful in the summer due to the open nature of the icepack.

TABLE OF CONTENTS

LIST OF FIGURES

LIST OF TABLES

ACKNOWLEDGEMENTS

I would like to thank a number of individuals and organizations that have provided me with the tools and assisted me with my efforts to make this research a success. First and foremost, my deepest gratitude is extended to Professor Robert H. Bourke for his support and guidance. His availability and willingness to extend his work day for me was greatly appreciated. Dr. Peter Guest was also instrumental as my second reader as he provided timely advice to ensure that the effects of atmospheric forcing was correctly portrayed in this research. Dr. Jim Wilson added background and perspective for the ambient noise problem in the Arctic and was very helpful as an additional second reader. The entire faculty and staff of the Department of Oceanography were a valuable resource for all of my concerns during the processing and interpretation phase of my research. In addition, I would like to thank the following individuals who provided me with essential data, expertise and assistance: Dr. Peter Stein of Scientific Solutions Inc. for providing the ambient noise data set, Dr. Ronald Kwok of the Jet Propulsion Laboratory for providing the RGPS data, and Ms. Pam Posey and Dr. Ruth Preller of the Navy Research Laboratory, who were especially helpful by promptly answering any requests for PIPS energy dissipation and NOGAPS model data. I would also like to thank the SHEBA Atmospheric Surface Flux Group, Ed Andreas, Chris Fairall, and Ola Persson for help collecting and processing the meteorological data used in this thesis. The National Science Foundation supported this research with grants to the U.S. Army Cold Regions Research and Engineering Laboratory, NOAA's Environmental Technology Laboratory, and the Naval Postgraduate School. Finally, I would like to thank my parents for their understanding and support during this past year along with my girlfriend, Ms. Andrea Krantz, who provided organizational assistance and tolerated busy weekends and conversations preoccupied with my thesis.

I. INTRODUCTION

A. HISTORY AND BACKGROUND

1. Background

Knowledge of the ocean environment has been a major consideration of the U.S. Navy since Commander Matthew Fontaine Maury began studying the Navy's pre-Civil War hydrology charts. The emergence of unrestricted submarine warfare during the world wars resulted in a "substantial broadening of the scientific disciplines needed in the practice of oceanography for naval applications" (Oceanographer of the Navy, 2000). These studies of underwater acoustics were naturally focused on areas of likely future combat.

During the 1980s and early 1990s, the former Soviet Union made substantial gains in submarine propulsion that resulted in a significant decrease in radiated noise production of Soviet, and now Russian, submarines. The continued deployment of Russian nuclear ballistic missile submarines in the Arctic Ocean necessitates that United States submarine crews be highly knowledgeable of the acoustic attributes of the polar ocean.

Ever since the USS Nautilus (SSN-571) made its historic voyage to the North Pole in 1958, U.S. submarines have operated in the ice-covered Arctic Ocean. The under-ice acoustic environment presents unique sonar problems, many of which have yet to be solved. Among these is the need to create an accurate Arctic ambient noise prediction model, a goal of U.S. Navy researchers for the past 25 years. Unlike mid-latitude ocean environments, ambient noise levels observed in the ice-covered Arctic are highly variable (as much as 20-30 dB over several hours), which exerts a significant effect on sonar performance and detection range. Therefore, the effect of extreme noise events is key to understanding the noise field of the Arctic Ocean.

2. Prior Investigations

Past ambient noise research efforts in the Arctic have attempted to correlate low to mid-frequency (< 600 Hz) ambient noise with local parameters, such as wind speed and ice speed (Buck and Clarke, 1989; Lewis and Denner, 1988; Dyer, 1988), but were mostly of limited success due to the influence of distant noise sources propagating with little attenuation to receivers well removed from the noise source. The research in this thesis presents a more basin-wide and dynamic approach to this problem. Using plots of energy dissipation and ice deformation, respectively, from the Polar Ice Prediction System (PIPS) and Radar Satellite Geophysical Processor System (RGPS), the location of noise sources (i.e., storm centers) can be identified and their noise intensity roughly estimated as a function of range. Since the ambient noise measured at any point is the sum of the contributions from all noise producing phenomena in the surrounding area (taking source level and transmission loss into account), the contribution from remote sources as well as local noise sources is required in order to increase correlation and predictive accuracy. Therefore, the potential of RGPS and PIPS as inputs to a future ambient noise model must be evaluated.

Recent studies of the synoptic atmospheric patterns of the Beaufort Sea have recognized a 10-15 year oscillation between predominantly cyclonic and anti-cyclonic motion in the sea level pressure pattern (Proshutinsky, 1997). The Beaufort Gyre heavily influences the region of the SHEBA experiment and, since the gyre is predominantly

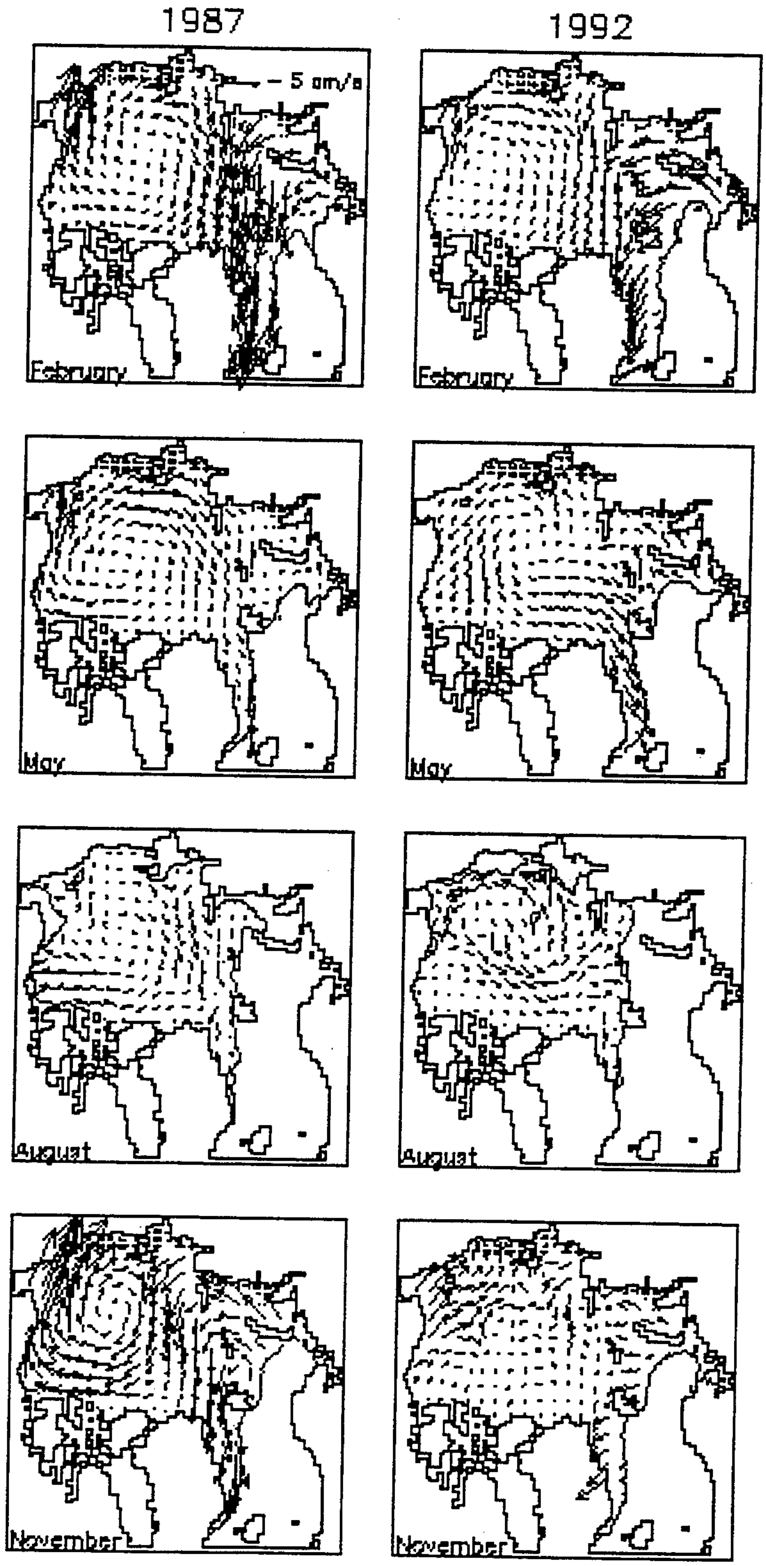

Figure 1. Seasonal variability of the ice drift and ice edge location (solid line) in 1987 (anti-cyclonic regime) and 1992 (cyclonic regime). Dotted areas depict location of fast ice (from Proshutinsky et al., 1999).

wind driven, the change from a cyclonic to an anti-cyclonic regime exerts a substantial impact on the motion and intensity of the gyre as shown in Figure 1. The Beaufort Gyre was under the influence of an anti-cyclonic mode from 1972-79, a cyclonic mode from 1980-1983, an anti-cyclonic mode from 1984-1988, and a cyclonic mode from 1989 until the present (Proshutinsky, 1997). Anti-cyclonic regimes have resulted in colder, drier years with a more convergent and consolidated year round ice pack. Cyclonic regimes are associated with warmer atmospheric temperatures, an increase in cyclonic storm activity (mostly arriving from Siberia), divergence of the ice cover and subsequent thinning of the ice pack (Polyakov, 1999). The latter two factors are conducive to a reduction in ice-generated noise levels. Most of the past ambient noise investigations in the Beaufort Sea were conducted during anti-cyclonic regimes, making the SHEBA noise data especially valuable as it is the only recent data set representative of conditions prevalent during a cyclonic regime.

During the extended cyclonic regime of the 1990s, there has been a strong downward tendency in total ice extent in summer (Maslanik, 1999). This trend has been especially evident in the Beaufort Sea and Chukchi Sea region. While satellite-observed ice cover has fluctuated over the past 40 years, 1998 emerged as a record year for ice reduction (see Table I) in the west Arctic. The low ice coverage of 1998 was at least in part due to preconditioning caused by the record reduction in ice coditions noted by McPhee et al. (1998) during the summer of 1997. This general decrease in ice thickness and concentration most likely was manifested in a high sensitivity of the pack to wind forcing (Maslanik, 1999), which is traditionally highly correlated with ambient noise.

Year	Western Arctic Extent
1998	0.77
1958	1.02
1993	1.04
1997	1.08
1979	1.09
1968	1.12
1977	1.12
1973	1.16
1982	1.16
1995	1.18

Table I. Ranking of years with minimum ice extent at the end of September for the western Arctic Ocean. Ice extent (10^6 km^2) are calculated based on areas with at least 20% ice concentration. The 46-year mean (1953-1998) for the Western Arctic is 1.25 x 10^6 km^2 (from Maslanik, 1999).

B. PURPOSE

Considering the needs of the naval forces operating in the Arctic and the scientific community in general, this thesis has two distinct objectives.

The first goal was to characterize the ambient noise field in the Beaufort Sea during a period of strong cyclonic forcing. This presents an opportunity to contrast the SHEBA noise data with previous investigations in the Beaufort, which were all conducted during an anti-cyclonic atmospheric pressure regime.

The second goal was to determine the value of PIPS and RGPS as dynamic inputs for an ambient noise model. By examining their output during extreme ambient noise events, one may assess their strengths and weaknesses as a tool for ambient noise source interpretation and forecasting.

THIS PAGE INTENTIONALLY LEFT BLANK

II. AMBIENT NOISE, METEOROLOGICAL, AND POSITION RECORDS

The data recorded during the SHEBA project were collected from three distinct sites. The two ambient noise records were recorded by two separate, ice-mounted buoys, which drifted with the ice from October 1997 through August 1998. The meteorological data were recorded at the main SHEBA site nearby the ice-bound Canadian icebreaker *Des Groseilliers.* The buoys were originally positioned north and east of the ship at distances of 50-60 km (see Figure 2). The distance from the buoys to the ship gradually increased throughout the measurement period so that most summer observations were taken about 100 km from the ship (see Table II and Figure 3).

The first full day of ambient noise recording for both buoys was 08 October 1997 (282)[1]. Operations continued until 01 December (336) when Buoy 2 failed. From 15 October 1997 (289) until the termination of the winter data on 01 February 1998 (396), an unknown error corrupted the data from Buoy 1 such that high frequency noise data were highly correlated with low frequency data. Buoy 2's data did not reflect this error, so it was assumed that there was a technical fault with Buoy 1. Hence, during the winter period, only low frequency data (160 Hz and below, based on the frequency correlation results) were used for Buoy 1's noise analysis. After 01 February 1998 (396), no ambient noise or position data were recorded for either buoy until 24 May (510) when both buoys were recovered and serviced by the SHEBA relief crew and recordings started again. Unfortunately, for the first 35 days of this period an unknown malfunction produced erred data that was omitted. Data collection resumed on 28 June (545) when Buoy 1's

[1] Julian date. All julian dates are referenced to 1 Jan 97 as being day 1 and 1 Jan 98 as being Day 366.

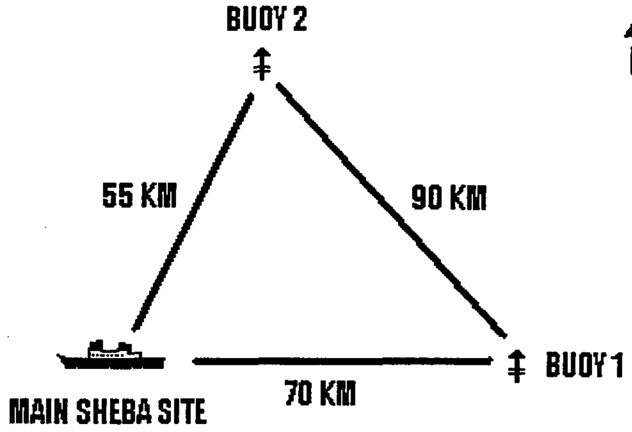

Figure 2. Placement of the two ambient noise buoys in relation to the icebreaker *Des Groseilliers* (main SHEBA camp).

	BUOY 2	SHIP
BOUY 1	Leg 1: 87.2 Leg 2: 47.0 Leg 3: 46.6 Leg 4: 46.8	Leg 1: 68.7 Leg 2: 73.4 Leg 3: 72.3 Leg 4: 90.1
BUOY 2	X	Leg 1: 52.0 Leg 2: 99.3 Leg 3:108.6 Leg 4:115.0

Table II. Separation distances (in kilometers) between the two buoys and between each buoy and the ship (main SHEBA camp).

hydrophone was replaced. From this time until the termination of the experiment on 10 September 1998 (619), the ambient noise record of both buoys was essentially free of errors or missing data.

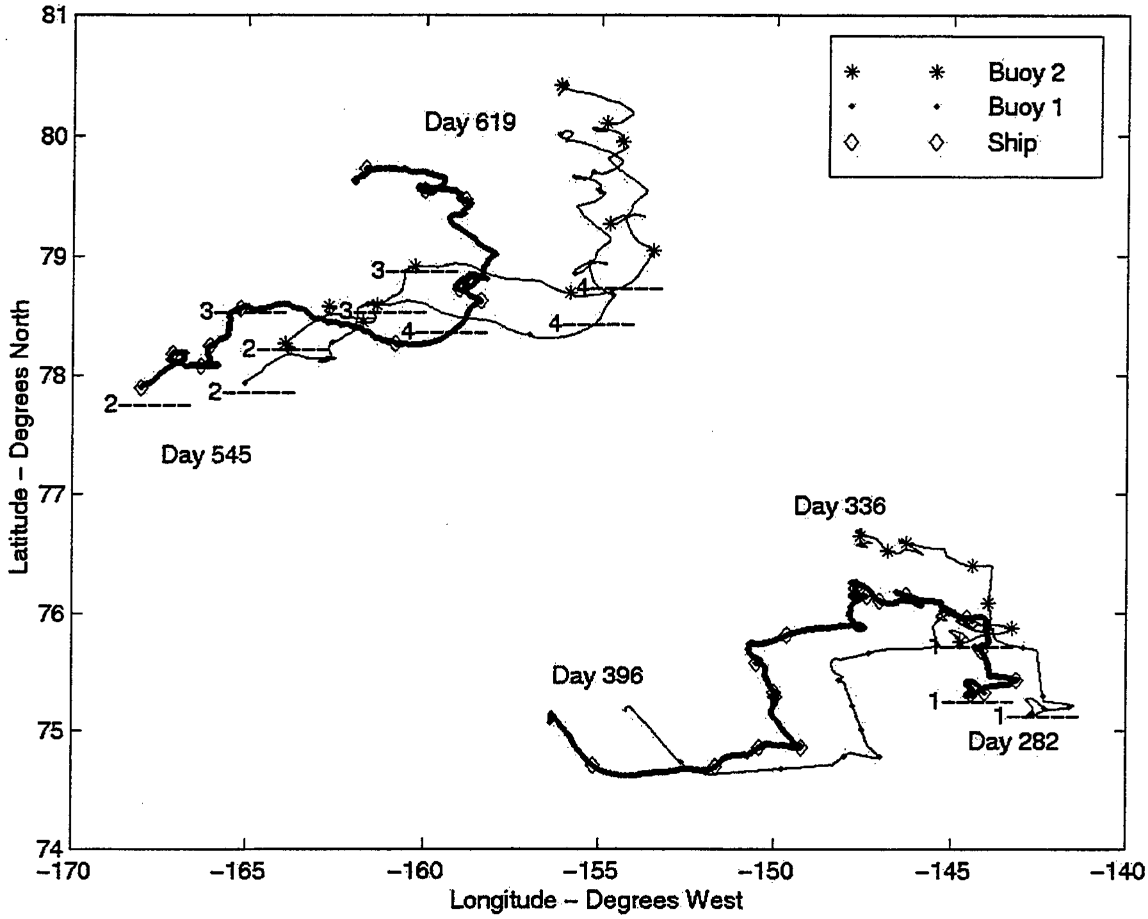

Figure 3. Drift tracks of the two buoys and the *Des Groseilliers* from October 1997 through September 1998.

A. BUOY/METEOROLOGICAL CHARACTERISTICS AND BACKGROUND

The buoys measured the noise field at 19 frequencies of which 14 were utilized in this study. The 14 frequency bands were one-third octave wide and centered at 50, 80, 100, 125, 160, 200, 250, 320, 400, 500, 640, 800, and 1000 Hz. Noise measurements were made on the hour and data was transmitted via ARGOS. Sampling was done at 8 kHz using an 8086 in-buoy processor to create hourly-averaged voltages for each one third-octave band. Sampling of the noise field was performed for about 0.5 sec, then processed for about 0.5 sec, then repeated a total of 20 times per hourly observation such that each hourly observation represented a 10-second sampling interval.

During the yearlong SHEBA experiment, the SHEBA Atmospheric Surface Flux Group acquired over 30 billion meteorological data points. The meteorological measurements of wind speed, surface momentum flux and air temperature were sampled 20 times per second. They were then averaged per minute and eventually averaged per hour. The time of each hourly value corresponds to the preceding 60 minutes of averaged observations (i.e., 0700Z – 10 knots indicates a 10 knot wind value averaged from observations between 0600 and 0700).

The momentum flux was determined by utilizing three sonic anemometers that measured the wind speed aligned along a 3-component axis system. The u-component was defined as being in the direction of the wind; the v and w-components were perpendicular to the wind in the horizontal and vertical directions, respectively. The instantaneous u, v, and w-components were averaged over a five-minute period to determine a mean value from which the wind speed fluctuations (u', v', w') could then be measured with the same sampling rate as the wind observations (Guest, personal communication).

B. PREPARATION OF NOISE DATA

The ambient noise data were recorded as voltage fluctuations that were converted to dB re: 1 $\mu Pa^2/Hz$ by first subtracting 22 dB to account for the filter/preamp gain in the system and then adding 141 dB to account for hydrophone sensitivity. Therefore, the net conversion added to the voltage data was 119 dB. The data were then corrected for bandwidth. For each one-third octave center frequency listed above, a constant of 10 log (bandwidth) was subtracted to correct for bandwidth differences (Kinsler et al., 1982).

The noise records were then edited for bad and missing data. Bad data were initially defined as noise levels louder or quieter than three times the standard deviation from the mean of the entire noise record. The data were then interpolated linearly to fill missing or bad data and to establish a corrected hourly time series. The percentage of missing and bad data varied from 6-10% in the winter of 1997 to 2.5-7% after May 1998. The majority of the interpolated gap lengths were quite short, only one to three hours. A summary of the interpolated gap lengths appears in Table III. In Buoy 1's record, one 79-hour gap was interpolated and used during data analysis. Buoy 2's record included seven gaps of four to ten hours of duration that were also interpolated and analyzed. However, the interpolation of very large data gaps (over 200 hours) that occurred in the ambient noise records were not included in the data analysis, so that only the data preceding and following the large gaps were compared. After the interpolation, another

LEG NUMBER	BUOY 1		BUOY 2	
	Gap Length (Hours)	# of Occurrences	Gap Length (Hours)	# of Occurrences
ONE	1	61	1	39
	2	1	2	3
	4	1	3	2
	6	1	4	2
	79	1	6	1
			7	1
			8	1
			9	1
			10	1
TWO	1	4	1	22
THREE	1	2	1	7
			2	1
FOUR	1	11	1	16
	2	1	2	3
			3	1

Table III. Lengths (in hours) of gaps in the noise data record.

check was made to ensure that the interpolated values did not exceed three times the standard deviation from the mean. To further remove outliers, values that exceeded twice the standard deviation from the mean were examined manually for continuity. The manual check ensured that data points were not rejected due to a large or small trend in decibel level, but were actually single point outliers. Removals due to outliers were then replaced by linear interpolation. A summary of the data statistics is presented in Appendix A.

Buoy 1's malfunctioning hydrophone was replaced as a stop-gap measure by a similar but non-calibrated hydrophone. Analysis of the summer noise record revealed that it was consistently recording values about 10-15 dB lower than that of Buoy 2. In an attempt to apply a reasonable calibration to this hydrophone, the amplitude of Buoy 1 relative to Buoy 2 was examined using the first week of winter noise data since the first seven days of Buoy 1's winter data were not corrupted. This week long record indicated the noise levels of the two buoys, only 87 km apart, were within 1-1.5 dB of each other. This noise difference was also calculated for only the low frequencies for the entire winter data set (note that frequencies of 160 Hz and below were determined to not be corrupted as stated above) and it was found to be similar to the low frequency, weeklong calculations. Therefore, based upon the first week's winter data, a calibration constant was computed for each frequency and added to Buoy 1's summer noise data in order to establish the same relative amplitude for the summer noise data as for the winter data.

C. PREPARATION OF METEOROLOGICAL DATA

The meteorological data were collected at a 20-meter tower one-kilometer from the main SHEBA site. The SHEBA Atmospheric Surface Flux Group edited the wind data for outliers. A moving filter removed outliers before computing the short-term averages used to determine the hourly value (Guest, personal communication).

The surface momentum flux was determined by first performing a coordinate rotation to align u with the wind direction and then correlating the horizontal fluctuation values with the vertical fluctuation values ($\overline{u'w'}$, $\overline{v'w'}$). The friction velocity (u_*) was then computed by taking a vector mean of the two correlated values ($\overline{u'w'}$, $\overline{v'w'}$) as shown in the following equation:

$$u_*^2 = \sqrt{(\overline{u'w'})^2 + (\overline{v'w'})^2}$$

Wind stress (τ) was then determined by

$$\tau = \rho(u_*)^2$$

where density (ρ) is determined by the virtual air temperature and pressure at the tower (Guest, personal communication).

Gaps in the wind data were initially interpolated linearly. When correlated with the ambient noise record, the linearly interpolated wind speed data lead to correlation values of 0.4-0.5 in the winter and 0.55-0.65 in the summer. The low winter correlation levels were primarily due to frequent but short-term data gaps in the wind time series caused by icing of the anemometers. Three of the winter gaps were greater than 24 hours. An attempt was made to improve on the linear interpolation by filling data gaps using the well-known relation between wind speed and ice speed first postulated by Nansen during his epic voyage on the *Fram* in 1893. This relation indicates that the ice speed moves at 2% of the surface wind speed. The method was later confirmed by the measurements made during the AIDJEX experiment in the Beaufort Sea in 1976 (Lewis and Denner, 1988). Strong confidence can be placed in this relation because at the SHEBA site the correlation between wind speed and ship drift speed was approximately 0.80. The ship drift speed was determined by taking the derivative of the hourly position time series of the ice-locked *Des Groseilliers,* which was established by running a cubic spline through the 4-hourly ship's log position reports as determined by the Global Positioning System (GPS). By inserting the ship drift speed-derived wind estimations into the data gaps of the wind speed time series, the correlation of wind speed to ambient noise improved to 0.55-0.60 in the winter and 0.60-0.80 in the summer. Of the wind speed data gaps, 70%

were 3 hours or less. A large gap of 350 hours during the winter was not analyzed as only the data before and after this gap was utilized. A summary of the wind data gaps is presented in Appendix A.

D. PREPARATION OF POSITION DATA

The ship and noise buoy position data were recorded via satellite. A GPS position report was recorded every 12 hours for the two buoys and every 4 hours for the ship. The ship data were taken from the ship's bridge log and then interpolated hourly using a cubic spline. The buoy position data were checked for errors by manual comparison of the drift track of each buoy and the ship. The buoy position reports were linearly interpolated and then re-examined for errors not evident before interpolation.

The tracks were divided into four legs (Figure 3). Leg 1 is representative of winter data recorded early in the SHEBA exercise when the drift track was predominantly west and northwest. Legs 2, 3, and 4 occur consecutively during the following summer. Leg 3 was isolated as a unique segment of the summer drift track as it showed evidence of a significant change in the drift pattern due to forcing by a strong cyclonic storm.

Due to the high correlation of motion between the two buoys, movement data from one buoy was used to help fill significant regions of poor and missing data in the other buoy on two occasions. In Leg 1, five position reports from buoy 2 were used to interpolate erred position reports noted in buoy 1. In Leg 4, three position reports from buoy 1 were used to interpolate erred position reports noted in buoy 2.

E. OTHER DATA SOURCES

Radar Satellite Geophysical Processor System (RGPS) data were provided from the Jet Propulsion Laboratory in Pasadena, CA (Kwok, personal communication). RGPS is a sophisticated computer system that compares Radar Satellite (RADARSAT) Synthetic Aperture Radar (SAR) images of Arctic sea ice recorded one to three days apart and creates geophysical products such as sea ice motion, thickness distribution of new ice, and backscatter history of the ice (Kwok, 1997). The RGPS products were used to determine areas of convergence and divergence of the sea ice cover. This information was presented in a gridded, color output to be used for the analysis of sea ice deformation in the SHEBA locale.

Polar Ice Prediction System (PIPS) data were provided by Ms. Pam Posey of the Naval Research Laboratory (NRL) at the Stennis Space Center, Louisiana. Color plots of energy dissipation (q is in units of milli-Watts/m^2) across the Arctic Basin were provided twice daily throughout the entire SHEBA time frame. If q is taken to be the rate of work done by the stress (σ) during plastic stretching (ε) (Pritchard, 1980), then:

$$q = \sigma_I \varepsilon_I + \sigma_{II} \varepsilon_{II}$$

where ε_I is the dilatation rate or time rate of change of the ice area and ε_{II} is the maximum shearing rate or time rate of change due to shear.

Using principal components:

$$\varepsilon_I = \varepsilon_{11} + \varepsilon_{22} \text{ and}$$

$$\varepsilon_{II} = 2\left[\frac{(\varepsilon_{11} - \varepsilon_{22})^2}{4} + (\varepsilon_{12})^2\right]^{1/2}$$

The PIPS output of total energy dissipation ranges from 0-30 milli-Watts/m^2.

III. NOISE, METEOROLOGICAL AND POSITION DATA ANALYSIS

A. SHIP-BUOY SPATIAL COHERENCY

1. Buoy and Ship Drift Cross-Correlation

Since the meteorological data and the ambient noise data used in this study were recorded at separate locations (60-100 km apart, see Table II), an analysis was conducted to determine the effect this separation may have had on the cross-correlation values. A strong correlation is noted between the motion of each buoy and between each buoy and the ship, during both summer and winter seasons (Table IV). Correlations of ice motion in excess of 0.7 and 0.8 for Buoy 1 and Buoy 2, respectively, versus the ship are noted in winter when the ship was approximately 60 km from the buoys. The correlation between the two buoys is further testament to the contiguous nature of the winter icepack as it exceeded 0.8 over the buoy separation distance of over 80 km. The summer months exhibited similar high correlations (greater than 0.8) between the buoys and the ship, even though a more independent motion would be expected due to the marked reduction in ice concentration during the summer months (Figure 4) and the increased separation distance (approximately 100 km) between the buoys and the ship. This would indicate that the maximum separation distance between the buoys and the ship during the experiment (115 km) was well within the correlation length scale. The relative motion of the two buoys was highly correlated during the summertime (0.95), which is explained by their close proximity (approximately 45 km) during this time.

	Buoy 1 vs. Buoy 2 (cor/lag)	Buoy 1 vs. Ship (cor/lag)	Buoy 2 vs. Ship (cor/lag)
Winter	0.82/0	0.73/+1	0.81/+1
Summer	0.95/0	0.83/+1	0.80/+1

Table IV. Correlation of the ice drift speed of the buoys and ship.

The response of the buoys to external forcing was nearly simultaneous as the lag of their motion was zero. However, the motion of the buoys consistently lead the motion of the ship by an hour. Because the buoys remained to the north and east of the ship throughout the yearlong drift period, the lag times imply that external forcing arrived from the northeast quadrant and influenced the buoy drift pattern about an hour before exerting a similar influence on the ship motion.

2. Ice Motion/Wind Speed Correlation

The buoy and ship speeds were also cross-correlated with the wind speed (Table V). As the meteorological data were collected near the ship (within 1 km), the correlation between wind and ship drift speed was expected to be quite high and was found to be essentially independent of season (i.e., degree of ice cover), varying from 0.82 to 0.84. The winter SHEBA wind speed record and the buoy position records (particularly Buoy 1) contained more linearly interpolated data than the summer records, which may account for the slight decrease in the winter correlations when compared to summer. Overall during the winter, the buoy drift and wind speed correlations compare very favorably with the correlations between the ship drift and wind speed, which would suggest that during the winter the distance between the buoys and the ship was well within the correlation length scale.

	Buoy 1 (cor/lag)	Buoy 2 (cor/lag)	Ship (cor/lag)
Winter	0.75/-2	0.80/-3	0.84/-1
Summer	0.83/-2	0.81/-2	0.82/-2

Table V. Correlation of the ice drift speed of the buoys with wind speed.

The drift speed of each buoy during summer was remarkably well correlated with the wind speed (values in excess of 0.8) even though in summer the buoys were at a greater distance from the ship. Since the ice concentration was particularly low in this part of the Beaufort Sea during the summer of 1998 (6-7 tenths coverage, see Figure 4), the buoy motion most likely approximated a free drift condition such that the internal stress of the ice was negligible when compared with the wind stress. Therefore, at the hourly sampling rate, the ice was predominantly wind driven during this period. Because the cross-correlation values of the buoy drift speeds were nearly identical to that for the ship (see Table III), it would seem that the wind velocity recorded at the SHEBA site was indicative of wind forced motion extending well beyond the ship, certainly to distances greater than the 100 km ship-buoy separation distance.

The lag times of the cross-correlation between wind and ice speed indicate that the wind speed lags buoy motion by about two hours. Once again, due to the buoys' position, this implies that wind events arrived from the north and east with the buoys experiencing the effects of the wind about two hours before the ship.

B. NOISE ANALYSIS

1. Noise Spectra

The first step in the analysis of the ambient noise field observed during the SHEBA experiment was to examine the spectral levels measured by the two buoys. Median spectral levels were chosen as the measure of central tendency. In addition, noise levels at the 5th and 95th percentiles were determined to establish the characteristics of the noise field during extremely quiet or loud noise events. The spectral plots were partitioned into winter (October through February) and summer (June through September) periods in order to examine their seasonal noise characteristics (Figures 5 and 6).

After adjusting for calibration of Buoy 1, the low frequency noise spectra (<200 Hz) indicates a fair degree of consistency over the 60-120 km separation distance between the two buoys, with the low frequency amplitudes of Buoy 2 being greater than Buoy 1 by less than 1 dB. The summer low frequency median spectra were 3-5 dB quieter than winter levels. A reduction in under-ice noise level in summer in the central Arctic is a well-documented phenomenon (Buck and Clarke, 1989; Urick, 1983; Poffenberger, 1987; Oard, 1987), but the difference is often as much as 10-12 dB, considerably more than the seasonal difference noted in the SHEBA data. This reduction in the seasonal noise difference is most likely due to a significant reduction in 1997 winter noise levels, which may be ascribed to a lack of storms during the SHEBA year (Guest, personal communication). Fewer storms reduced the occurrence of convergent ice motion episodes and subsequent ridge building during the winter, which lead to depressed ambient noise amplitudes.

Summer noise levels did not decrease as noticeably due to the increased ice-ice interactions resulting from the record low ice concentrations.

The spectral slope was estimated to be –5 dB/octave, which is typical of the –5 to –6 dB/octave slope observed from over two decades of noise measurements from drifting buoys in the central Arctic basin (Buck and Wilson, 1986).

The noise spectra amplitude of Buoy 2 was about 2-3 dB greater than that of Buoy 1 at high frequencies (>200 Hz) during the summer (no winter data are available for Buoy 1 at high frequencies to make a similar comparison). As discussed earlier (e.g., Oard, 1987), local noise sources dominate at higher frequencies. During the summer, when local noise events are most common due to open ice conditions, noise spectrum levels can be expected to be highly variable and the 2-3 dB difference between buoys located 45 km apart seems reasonable.

The homogeneous nature of the noise field throughout the SHEBA area is also reflected in the standard deviation of the noise level recorded by each buoy. The standard deviation is often used as a measure of the noise field variability in response to multiple forcing mechanisms (Banister et al., 1979). In contrast to the CEAREX and ANMET experiments, the standard deviation for both buoys increased with increasing frequency. This would further substantiate that the noise field at low frequencies is strongly influenced by noise energy propagating from distant storms in the Arctic basin causing a relatively homogeneous noise field (i.e., levels centered near the median level) over a broad area. Typical values range from 3-4 dB in winter to 5 dB in summer. In contrast, high frequency noise is more variable, representing rather site-specific factors, especially given the degree of open water and thin ice conditions, with standard deviations of 6 dB being more common.

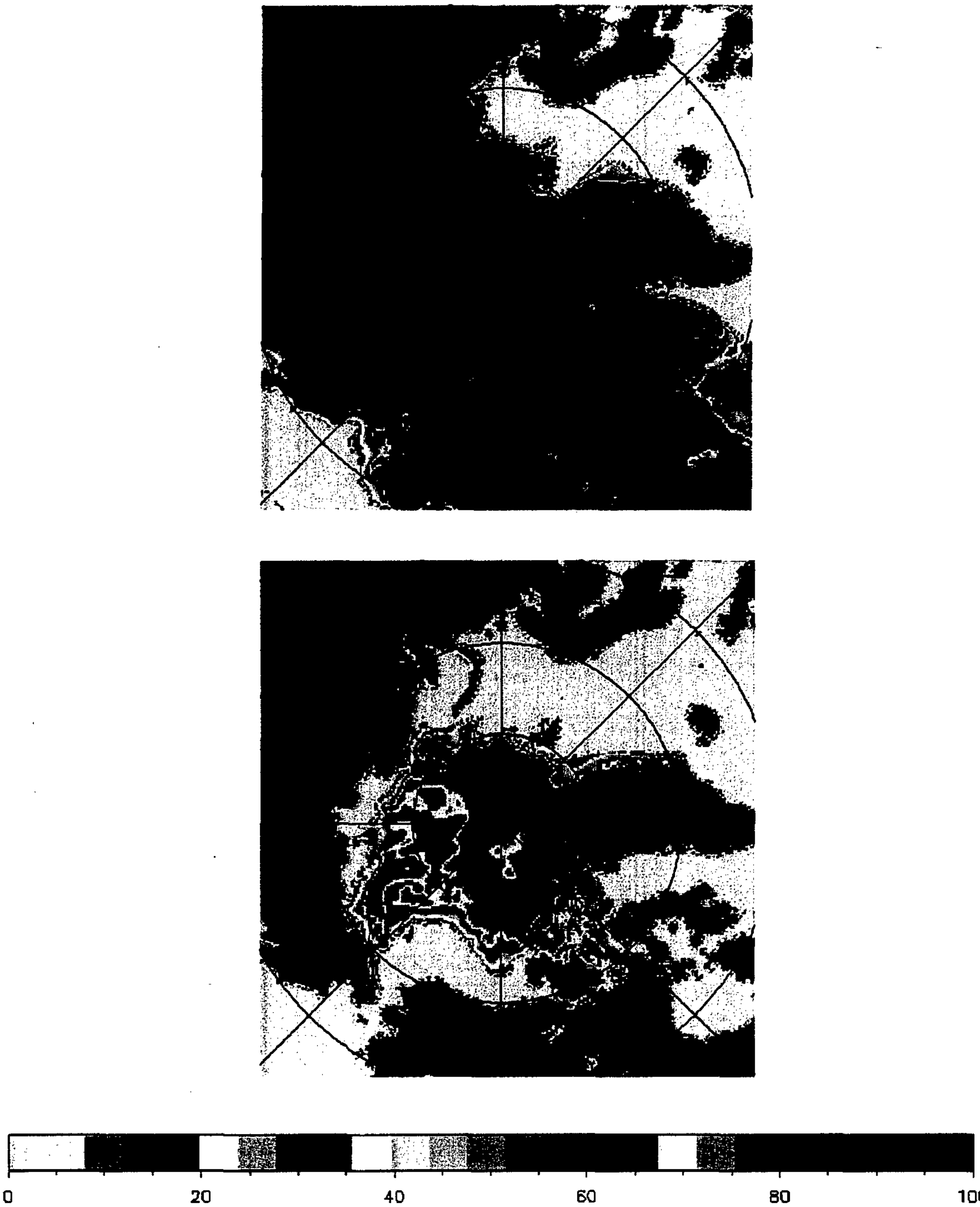

Figure 4. December 1997 (top) and August 1998 (bottom) monthly average ice concentration as determined by SSM/I NASA algorithm (from National Snow and Ice Data Center). The white circle indicates the position of the SHEBA camp.

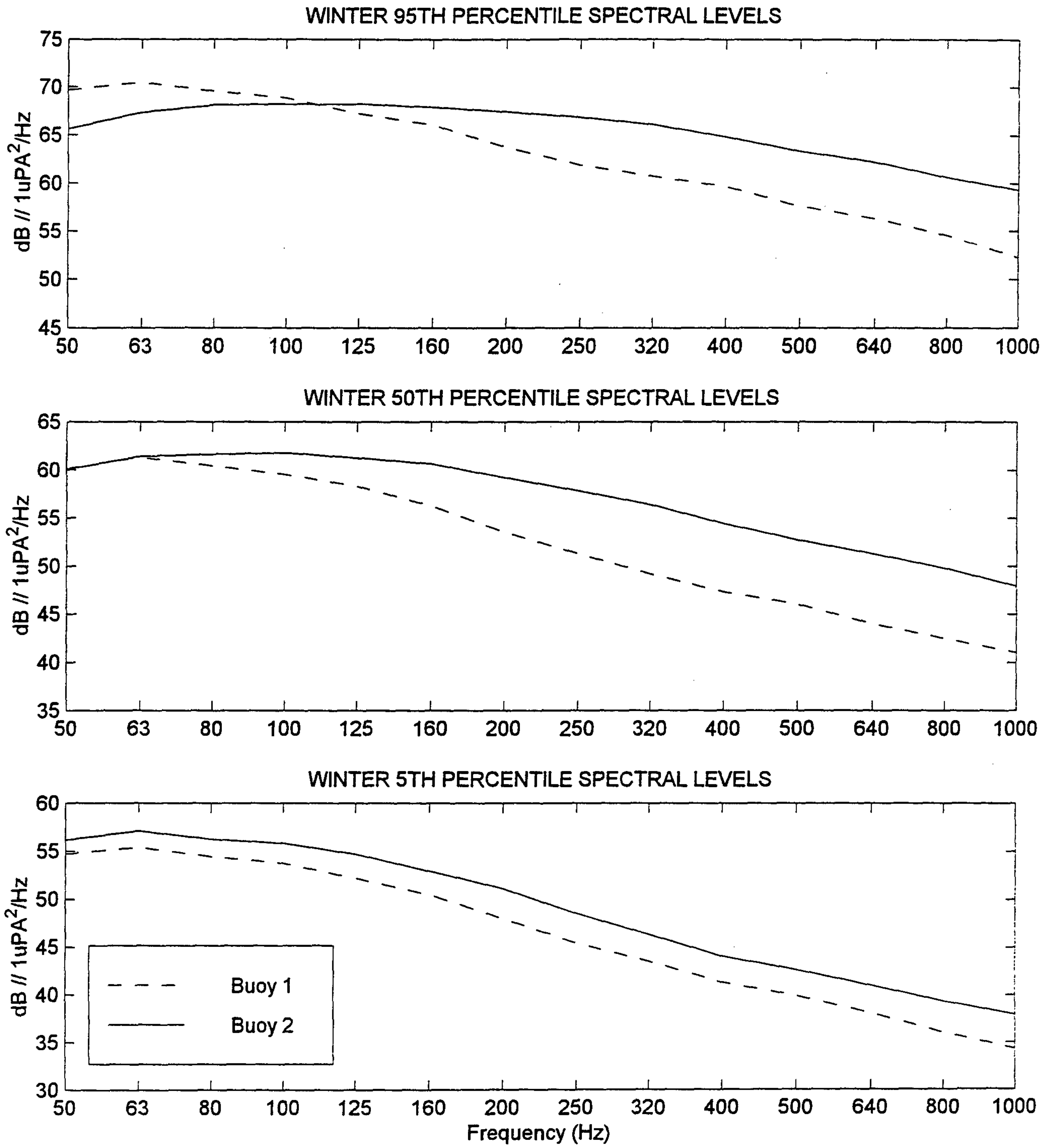

Figure 5. 95th percentile (top), median (middle) and 5th percentile (bottom) spectral levels for both buoys. Period covered is from 08 Oct 97 through 01 Dec97.

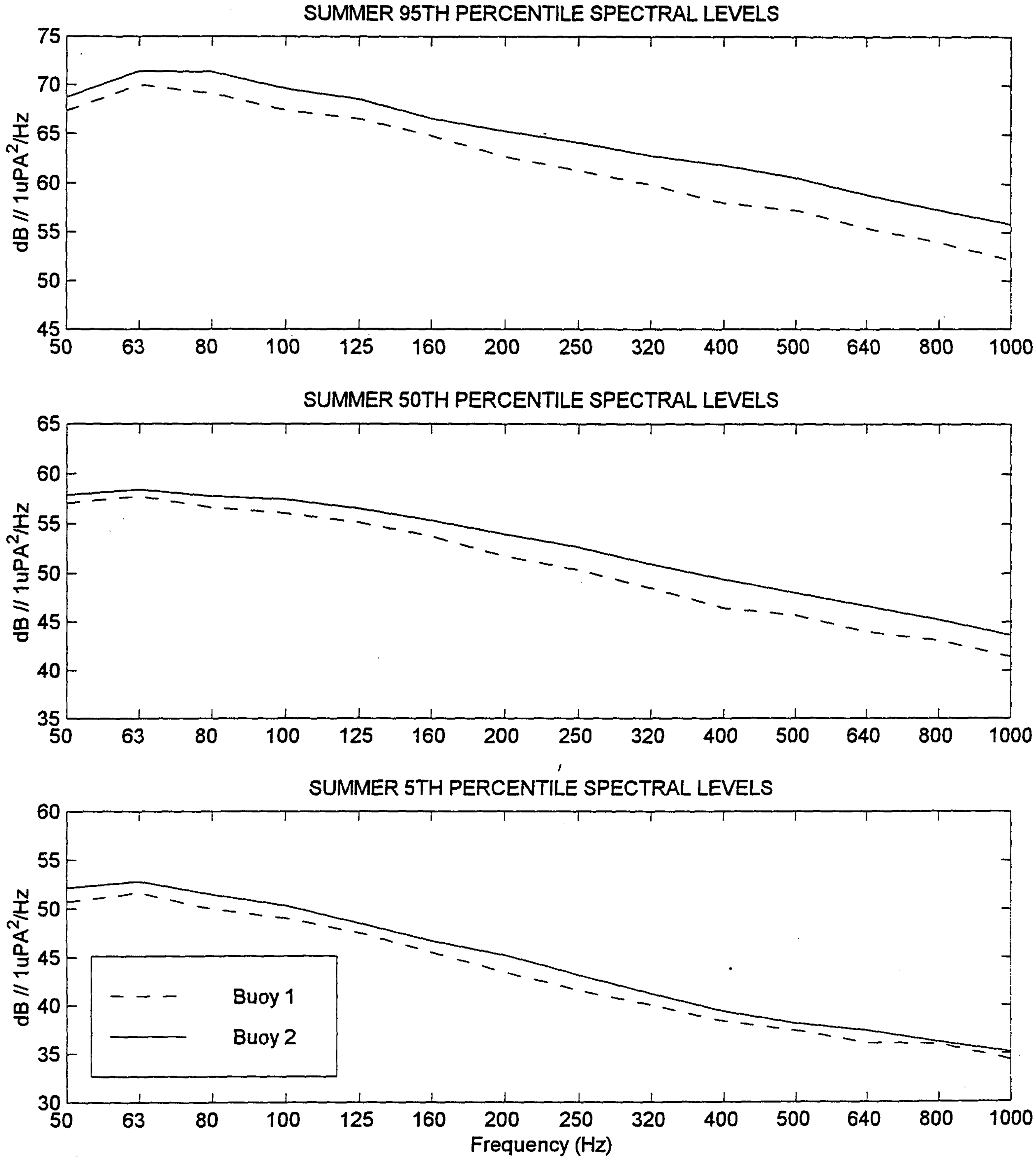

Figure 6. 95th percentile (top), median (middle) and 5th percentile (bottom) spectral levels for both buoys. Period covered is from 29 Jun 98 through 11 Sep 98.

2. Spectral Comparison With Past Investigations

The noise characteristics from the SHEBA data can be placed in perspective by comparison with spectra from other investigations in the vicinity of the Beaufort and Chukchi Seas. The noise data from previous studies were not partitioned by season, but represent median levels averaged over one to two years of 3-hourly observations. Buoy 2 was used for comparisons with past investigations as it contained the least interpolated and corrupted data (Table VI).

Study/Freq (Hz)	10	40	50	100	315	1000
1975-77 AIDJEX (Near 75° N)	X	X	X	50-62	X	X
AUG 1983-AUG 1984 (78-79° N)	75	73	X	67	59	X
APR 1985-FEB 1986 MAY 1985-JAN 1986 (82-82° N)	72-73	69-70	68-69	60-62	49-54	36-44
SHEBA OCT 1997-SEP 1998 (75-80° N)	X	X	W: 60.2 S: 58.7	W: 62.0 S: 58.2	W: 56.3 S: 51.3	W: 48.1 S: 44.2

Table VI. Comparison of the median noise record of Buoy 2 with past ambient noise studies in the Beaufort Sea.

Comparisons with past data must take into account the10-15 year oscillation of cyclonic and anti-cyclonic atmospheric pressure patterns that has recently been recognized in the Beaufort Sea region. The SHEBA data were collected during the end of the most recent cyclonic regime. The effect of cyclonic pressure regimes is most notable during summer months (see Figure 1) as anti-cyclonic pressure patterns are reinforced over the Beaufort Sea during the winters of cyclonic regime years (Proshutinsky and Johnson, 1997). This would suggest that anomalies in ambient noise would be most evident during summer months. The SHEBA data, being the only ambient noise data recorded during a cyclonic regime, reflected this trend as wintertime levels were comparable to past results. However, during the summertime, low frequency noise levels were clearly less than prior readings which were predominantly recorded during the summer months (see Table VI for dates of prior data), (Nordman, 1987). This is consistent with the concept that cyclonic regimes lead to extensive divergence of the ice pack and are likely to produce less ambient noise than periods of anti-cyclonic pressure when convergent conditions predominate (Bourke, personal conversation).

In contrast to the low frequency noise levels, the SHEBA high frequency noise levels were comparable to the past data. This may be due to the differing nature of the ice pack during a cyclonic or anti-cyclonic regime. During a cyclonic regime summer temperatures are warmer, producing more open water while at the same time, permitting an increase in the number of synoptic cyclones migrating through the Arctic. Both these factors lead to an increase in the number of high-energy ice-ice collisions, which lead to elevated levels of high frequency ambient noise. During an anti-cyclonic regime summer, colder temperatures limit the amount of open water while fewer storms penetrate due to the presence of the strong high-pressure cell. This leads to less ice divergence and more convergence, which is reflected in elevated noise levels. The high frequency noise produced by the high energy, ice-ice interactions of the cyclonic years seems to equate with the ambient noise generated by the convergence of the ice during anti-cyclonic years, leading to comparable high frequency noise levels during summer.

3. Temporal and Spatial Coherency

The temporal coherence, quantified by the e-folding time, is a measure of statistical independence of the noise field with time. The e-folding time is the time required for the autocorrelation coefficient to decay by a factor of e^{-1} (0.368). By computing the e-folding time, the temporal response of each hydrophone to a storm or forcing event can be deduced.

The e-folding times ranged from 6-26 hours, typically centered near 13-15 hours (Table VII). Similar to past studies throughout the Arctic Ocean, the winter e-folding times tend to decrease with increasing frequency in the winter (Bourke and Parsons, 1993) and increase with frequency during the summer (Bourke and Feller, 1999). Perhaps this is due to the extreme open nature of the summer ice, as mentioned in Chapter I, and the subsequent low ambient noise levels. Computations of the standard deviation during low noise periods (approximately 1-1.5 dB) during the summer showed little change in amplitude unless a large-scale event, such as a storm or direction change occurred. This is evident by examining the time series of the summer noise levels and the positions of the 5th and 95th percentile with respect to the median. The 5th percentile is 5 dB less than the median while the 95th is 18 dB

	Buoy #	**50 Hz**	**63 Hz**	**80 Hz**	**100 Hz**	**125 Hz**	**160 Hz**	**200 Hz**	**250 Hz**	**320 Hz**	**400 Hz**	**500 Hz**	**640 Hz**	**800 Hz**	**1000 Hz**
Winter	1	15	14	13	14	14	15	X	X	X	X	X	X	X	X
	2	13	10	9	9	9	9	9	8	9	7	6	6	6	6
Summer	1	15	15	14	13	14	14	18	20	23	23	26	26	26	26
	2	18	17	17	16	17	19	20	22	23	23	23	22	22	21

Table VII. Temporal coherency (e-folding time in hours) calculated from the autocorrelation function.

higher than the median. During winter records, the difference between the median and the 5th and 95th percentile is nearly equal. Therefore, it can be assumed that much of the summertime noise field consisted of extended periods of little noise level variation, which lead to an increase in the high frequency e-folding times.

In order to establish the spatial coherency of the noise field, a cross-correlation was performed on the ambient noise records of Buoys 1 and 2. Tables VIII, IX and X indicate a fairly high correlation existed between the two buoys during both winter and summer. The correlation was slightly higher during the summer due to the closer proximity (about 45 km) of the buoys compared to winter (85 km apart). The zero lag times throughout the record demonstrate that any forcing event effected both buoys within an hour, which, when considering the short separation distances, is consistent with the propagation speed (approximately 15-20 m/s) of central Arctic storms.

Frequency (Hz)	**Buoy 1 vs. Buoy 2**	
	Coef (max)	**Lag (hrs)**
50	0.91	0
63	0.87	0
80	0.84	0
100	0.79	0
125	0.78	0
160	0.74	0
200	0.66	0
250	0.60	0
320	0.55	0
400	0.55	0
500	0.55	0
640	0.55	0
800	0.56	0
1000	0.57	0

Table IXa. Maximum cross-correlation coefficients between the ambient noise records of the two buoys during the first week of the winter record (8 Oct 97 through 15 Oct 97).

Frequency (Hz)	Buoy 1 vs. Buoy 2	
	Coef (max)	Lag (hrs)
50	0.82	0
63	0.78	0
80	0.69	0
100	0.69	0
125	0.68	0
160	0.65	0

Table IXb. Maximum cross-correlation coefficients between ambient noise records of the two buoys during winter (8 Oct 97 through 1 Dec 97) for low frequency data (< 160 Hz).

Frequency (Hz)	Buoy 1 vs. Buoy 2	
	Coef (max)	Lag (hrs)
50	0.81	0
63	0.83	0
80	0.83	0
100	0.80	0
125	0.77	0
160	0.74	0
200	0.72	0
250	0.70	0
320	0.70	0
400	0.71	0
500	0.73	0
640	0.73	0
800	0.74	-1
1000	0.74	0

Table X. Maximum cross-correlation coefficients between the ambient noise records of the two buoys during the summer (29 Jun 98 through 11 Sep 98).

4. Environmental Cross-Correlations

The analysis of the relationship between the effects of wind and ice motion on the noise field was done by conducting a cross-correlation between wind speed, wind stress and ice speed against the noise level data from both buoys.

Although the surface wind speeds traditionally exhibit a high cross-correlation value when compared with ambient noise, the wind speed itself does not directly generate noise (Oard, 1987). For example, blowing snow can generate high frequency noise (Dyer, 1983). Wind stress is the means by which kinetic energy is transferred into ice motion, leading to ice-ice collisions and subsequent fracturing of the ice, which are the main mechanisms for the generation of low to mid-frequency Arctic ambient noise.

Tables XI, XII and XIII show the environmental cross correlations for Buoy 2 during different seasons and wind events. The Buoy 1 correlations demonstrated a similar trend. Similar to past studies (Bourke and Feller, 1999; Parsons, 1992), peak coefficients are greater at low frequencies (<200 Hz) in winter and greater at high frequencies in summer.

As stated earlier, the wind speed and momentum flux (wind stress) instruments were not co-located with the ambient noise buoys, but were recorded 1 km from the ship and main SHEBA station, which were separated from the buoys by a distance of 40-80 km. The lag times with respect to wind speed and stress (1-4 hours) are comparable to the lag times of other studies in the Arctic (Feller, 1994, Parsons, 1992) where the wind speed measurements were also conducted at locations of approximately 100 km from the drifting buoys.

During the winter, the correlation values of wind speed and wind stress with ambient noise were virtually the same. Ambient noise lagged wind speed by 1-2 hours and wind stress by 3-4 hours.

Frequency (Hz)	Wind Speed		Wind Stress		Ice Speed	
	Coef (max)	Lag (hrs)	Coef (max)	Lag (hrs)	Coef (max)	Lag (hrs)
50	0.55	-1	0.54	-4	0.33	-7
63	0.53	-1	0.50	-4	0.31	-7
80	0.53	0	0.50	-4	0.29	-3
100	0.52	0	0.52	-3	0.26	-3
125	0.50	-2	0.50	-3	0.24	-3
160	0.49	-2	0.50	-3	0.21	-1
200	0.48	-2	0.50	-3	0.21	-15
250	0.46	-2	0.48	-3	0.20	-17
320	0.46	0	0.47	-3	0.20	-15
400	0.45	0	0.46	-3	0.21	-13
500	0.44	0	0.46	-3	0.22	-12
640	0.45	0	0.47	-3	0.20	-9
800	0.45	0	0.47	-3	0.23	-1
1000	0.47	0	0.49	-3	0.28	-1

Table XI. Maximum cross correlation coefficients between ambient noise and environmental parameters for Buoy 2 during the winter (8 Oct 97 through 1 Dec 97). Negative lag times indicate the noise lagged the forcing.

Frequency (Hz)	Wind Speed		Wind Stress		Ice Speed	
	Coef (max)	Lag (hrs)	Coef (max)	Lag (hrs)	Coef (max)	Lag (hrs)
50	0.54	-2	0.52	0	0.44	-3
63	0.51	-2	0.50	0	0.40	-3
80	0.50	-2	0.50	0	0.43	-3
100	0.54	-2	0.51	-1	0.46	-2
125	0.54	-3	0.51	-1	0.48	-1
160	0.55	-3	0.52	-1	0.50	-1
200	0.55	-3	0.52	-2	0.52	-2
250	0.56	-4	0.53	-3	0.54	-2
320	0.58	-4	0.53	-3	0.57	-2
400	0.61	-4	0.54	-2	0.58	-3
500	0.62	-4	0.55	-3	0.60	-4
640	0.61	-4	0.55	-4	0.60	-4
800	0.61	-4	0.55	-3	0.60	-3
1000	0.61	-5	0.55	-4	0.60	-3

Table XII. Maximum cross correlation coefficients between ambient noise and environmental parameters for Buoy 2 during Legs 2 and 4 (Summer). Negative lag times indicate the noise lagged the forcing.

Frequency (Hz)	Wind Speed		Wind Stress		Ice Speed	
	Coef (max)	Lag (hrs)	Coef (max)	Lag (hrs)	Coef (max)	Lag (hrs)
50	0.60	0	0.48	0	0.41	-3
63	0.63	0	0.51	0	0.36	-3
80	0.62	0	0.53	+1	0.39	-3
100	0.61	0	0.51	+1	0.45	-1
125	0.59	0	0.50	+1	0.49	0
160	0.56	-1	0.48	+2	0.52	0
200	0.55	-1	0.46	-3	0.55	-1
250	0.58	-1	0.49	-2	0.59	0
320	0.57	-1	0.47	-3	0.62	0
400	0.61	-3	0.50	0	0.65	-3
500	0.65	-3	0.55	-1	0.65	-3
640	0.65	-3	0.58	-2	0.65	-3
800	0.67	-3	0.62	-2	0.65	-3
1000	0.67	-3	0.61	-2	0.65	-3

Table XIII. Maximum cross correlation coefficients between ambient noise and environmental parameters for Buoy 2 during Leg 3 (Summer). Negative lag times indicate the noise lagged the forcing.

In summer, the correlations of wind speed and wind stress with ambient noise were also quite comparable. However, the lag time between wind speed and ambient noise was increased by 1-4 hours compared to the winter, with longer lags associated with higher frequencies.

Past investigations have shown that ambient noise is most strongly correlated with wind speed (Bourke and Feller, 1999, Bourke and Parsons, 1993). However, few of these studies have measured the momentum flux directly as was done at SHEBA. By necessity, these investigations had to derive wind stress from an area-wide average of the geostrophic wind speed (Bourke and Feller, 1999). The direct measurements of momentum flux recorded during the SHEBA experiment presented a unique opportunity to examine the local variability in wind stress. The results indicated that the wind speed correlations were only slightly higher (approximately 0.05) than the wind stress correlations with ambient noise during the summer, but were virtually identical (approximately 0.01-0.02) during the winter. The conclusion is that it is safe to use the wind stress derived from bulk parameters and the geostrophic wind speed with a stability dependent drag coefficient in lieu of directly measured wind stress. The small seasonal difference is likely related to the seasonal change in ice concentration. The wind stress is highly site specific and is governed by local ice conditions such as roughness or boundary layer heights, which change with the wind direction. The large summer ship-buoy separation distance (90-110 km) emphasizes this difference in local conditions along with the increased instability of the surface boundary layer during summer. In contrast, during the winter, when the ice pack is more contiguous, locally measured wind stress is applicable across a much larger region, producing higher correlation values with the ambient noise recorded at the buoys. Also, the strong stability of the surface boundary layer in winter would serve to decrease the drag coefficient and therefore increase the wind stress correlation with ambient noise (Guest, personal conversation).

The correlation of ambient noise with ice speed was much less (by 0.2-0.4) than the correlation with wind speed/stress during the winter. During the summer, the correlation improved such that high frequency correlation values were similar to those of wind speed/stress, but the low frequency correlation values continued to be approximately 0.1 less than wind speed/stress values. This low correlation with ice speed is similar to results determined during prior investigations (Bourke and Parsons, 1993). As the SHEBA drift track was almost exclusively over deep water, tidal forcing was not a factor in causing the low ice drift correlation. However, inertial forcing definitely effected the drift, especially during the summer period (Perovich et al., 1999), which may account for some of the low correlation between ice speed and ambient noise during the summer. In winter the low correlation may be due to periodic episodes of ice drift counter to the mean flow of the Beaufort Gyre. Such episodes occurred during the fall and early winter when cyclonic storms migrated into the Beaufort Sea and created week-long periods when the wind forcing was opposite to the mean flow direction of the gyre. This convergence of mean flow and wind forcing would generate periods of increased ambient noise concurrent with periods of reduced ice speed, lowering the overall correlation. This phenomenon will be examined in more detail during the mesoscale analysis in the next section.

In general, the wind speed produced the highest and most consistent correlations with ambient noise. Similar to past results (Bourke and Feller, 1994), the degree of wind forcing was demonstrated to be the prime indicator of ambient noise levels in deep-water regions.

5. Mesoscale Analysis of Wind Forcing and Ambient Noise

The drift tracks of the ship and the two buoys (Figure 3) appeared to be quite similar, as expected considering the high correlation between the buoys and ship drift speeds. As described in Chapter II, each track was segmented into four legs representative of seasonal and specific drift features. In anticipation that each leg occurred in response to a change in the long-term wind forcing, a stick plot of the wind velocity and buoy drift velocities is presented in Figure 7. For example, it is apparent that Leg 3, a period of rapid easterly movement, was strongly influenced by strong and steady wind forcing from the west. The statistics of the buoy and ship trajectories for each leg are listed in Table XIV. The distance for each leg is the distance between end points while the displacement speeds represents an overall vector mean speed determined from the net distance traveled during each leg. The mean ice and wind speeds are mean scalar values derived from hourly measurements. The results indicate a relatively low overall vector drift speed of 2-6 cm/s, reflective of a meandering daily/synoptic path, when compared to the mean scalar ice speed, which ranged from 7-9 cm/s in the winter to 12-16 cm/s in the summer. The exception to this trend was Leg 3, which experienced strong forcing from a large synoptic storm and a nearly linear drift path. Leg 3's mean vector drift speed was 12-13 cm/s, much closer to its mean scalar ice speed (14-16 cm/s) than other legs. Table XIV also lists median ambient noise levels at three representative frequencies (80, 200, and 800 Hz) to demonstrate the acoustic response during each leg.

During Leg 1 (October 1997 – February 1998) the buoys and ship drifted in a generally westward direction, but were influenced by numerous strong autumn storms (NOGAPS surface pressure charts) which periodically reversed the ice drift to the east during the first half of Leg 1. During the three months of winter, the mean wind speed was relatively high at 5 m/s, but because of the episodic changes in the wind direction, the vector mean ice drift was about half the scalar mean drift speed. As discussed in the preceding section, the cyclonic storms produced an eastward forcing, which was opposite to the general westward flow of the Beaufort Gyre in this region. Therefore, ice speeds were much less than what was expected for the high winds due to net vector addition with the mean flow. An example of this occurred in mid-November (Julian Date 315-321). The atmospheric pressure pattern (Figure 8) for this event indicates a strong cyclonic storm moving east across the Beaufort Sea

	LEG 1 JD: 282-396	LEG 2 JD: 545-571	LEG 3 JD: 571-582	LEG 4 JD: 582-619
Leg Duration (Julian Days)	B1: 282-396 B2: 282-336 Sh: 282-396 FF: 304-396	B1: 545-571 B2: 545-571 Sh: 545-571 FF: 545-571	B1: 571-582 B2: 571-582 Sh: 571-582 FF: 571-582	B1: 582-619 B2: 582-619 Sh: 582-619 FF: 582-619
Leg Distance (km)	B1: 386.5 B2: 129.3 Sh: 396.6	B1: 88.5 B2:100.6 Sh: 99.0	B1: 124.2 B2: 114.7 Sh: 117.4	B1: 182.6 B2: 185.9 Sh: 154.8
Number of Records	B1: 2739 B2: 1292 Sh: 2739 FF: 2210	B1: 632 B2: 632 Sh: 632 FF: 632	B1: 260 B2: 260 Sh: 260 FF: 260	B1: 884 B2: 884 Sh: 884 FF: 884
Mean Scalar Ice Speed (cm/s)	B1: 8.71 B2: 8.02 Sh: 9.02	B1: 7.37 B2: 7.41 Sh: 7.71	B1: 14.33 B2: 13.17 Sh: 15.95	B1: 11.57 B2: 11.37 Sh: 12.39
Mean Scalar Wind Speed (m/s)	5.14	3.83	5.29	4.88
Mean Vector (Displacement) Speed (cm/s)	B1: 2.58 B2: 2.65 Sh: 2.55	B1: 3.95 B2: 4.04 Sh: 4.10	B1: 13.27 B2: 12.26 Sh: 13.82	B1: 5.73 B2: 5.83 Sh: 4.74
Ambient Noise Median @ 80 Hz (dB)	B1: 60.60 B2: 61.62	B1: 57.20 B2: 56.80	B1: 55.31 B2: 57.60	B1: 56.70 B2: 58.29
Ambient Noise Median @ 200 Hz (dB)	B1: 56.55 B2: 59.19	B1: 52.80 B2: 52.30	B1: 51.00 B2: 55.70	B1: 51.60 B2: 54.60
Ambient Noise Median @ 800 Hz (dB)	B1: 45.90 B2: 49.80	B1: 43.20 B2: 44.21	B1: 44.50 B2: 47.30	B1: 42.70 B2: 45.01

Table XIV. Ship and buoy trajectory statistics partitioned by leg (B1-Buoy 1; B2-Buoy 2; Sh-Ship).

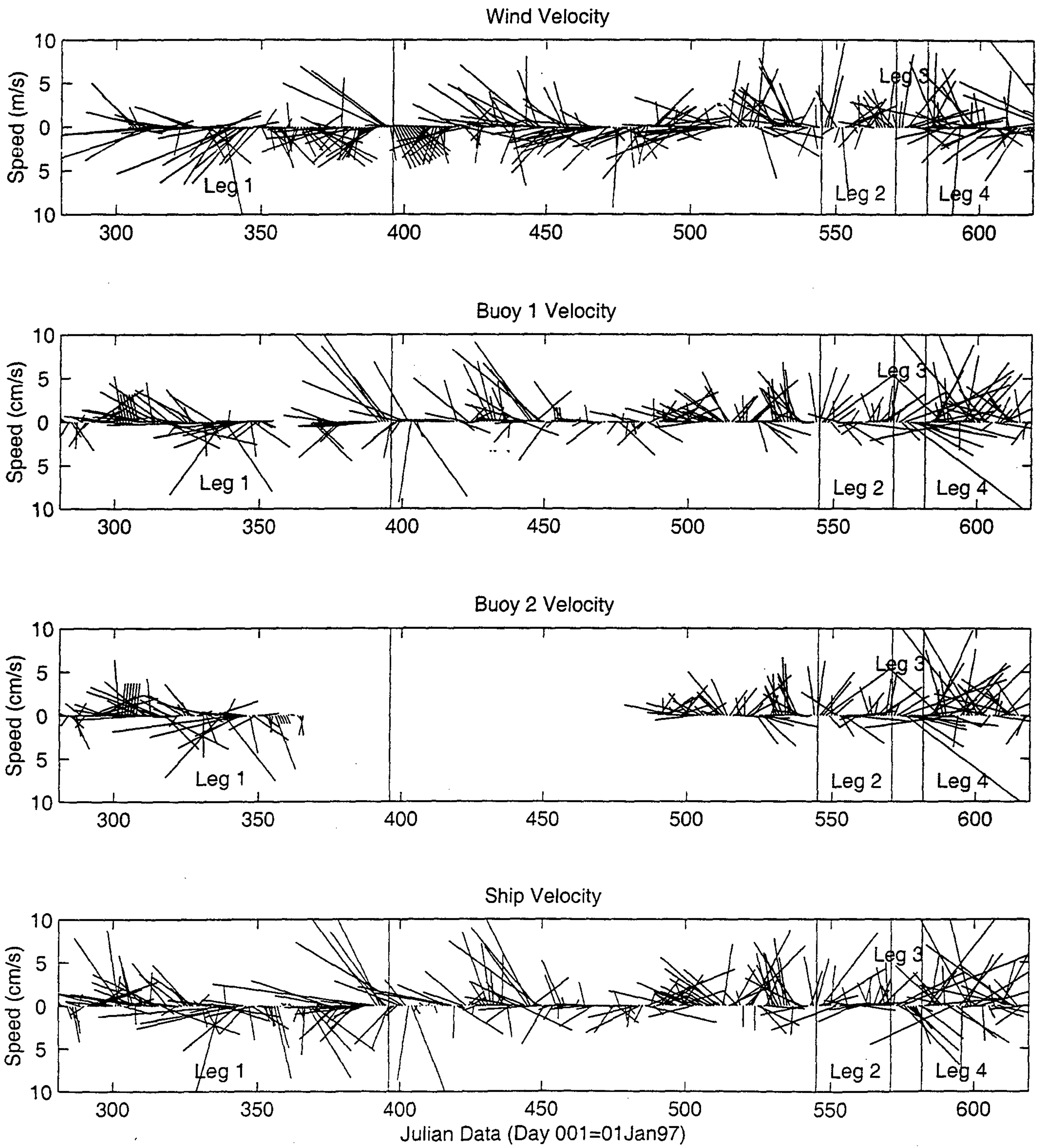

Figure 7. Stick plot of mean daily wind speed (measured near SHEBA camp) and ice drift speed from both buoys and the ship. Vertical bars represent boundaries between drift legs. All vectors point in the direction of motion in order to facilitate comparison.

from Siberia. The forcing from this storm is evident in the drift track of Buoy 2 (Figure 9) and in the strong westerly winds (10-13 m/s) experienced in the region. Buoy 2 experienced a moderate increase in ambient noise levels (Figure 9) during this period. This scenario occurred at least four more times during the autumn and early winter of 1997.

By late December, high pressure built into the area and dominated the region for the remainder of Leg 1. This served to strengthen the anti-cyclonic rotation of the Beaufort Gyre during the second half of Leg 1 and increased mean ice speed from 6.5 cm/s to 9.5 cm/s, even though the mean wind speed decreased from over 6 m/s to less than 5 m/s. The noise field responded with higher median low frequency levels (3 dB greater) during the first half of Leg 1 than the second half due to the convergent forces (wind forcing opposite to the mean flow direction) that acted on the ice. Due to the low transmission loss associated with low frequency propagation in the Arctic (Urick, 1983), the low frequency energy generated by the storms propagated over long distances, which increased the temporal range of the high noise level event at the buoys. In addition, the presence of autumn storms caused an increase in pressure ridge activity, which also would lead to increased low frequency noise levels.

Leg 2 (June-July 1998) began on June 28th, well into the summer melt season. A slow northeastward flow and strong inertial motion characterized this leg. It occurred during the calmest period of the investigation with mean wind and ice speeds much less than during the other legs and, as expected, the ambient noise during Leg 2 was the quietest recorded. The eddy-like motion of the drift track resulted in periods of strong convergence that contributed to low frequency noise levels (Bourke and Feller, 1999). However, the median high frequency noise levels clearly indicated

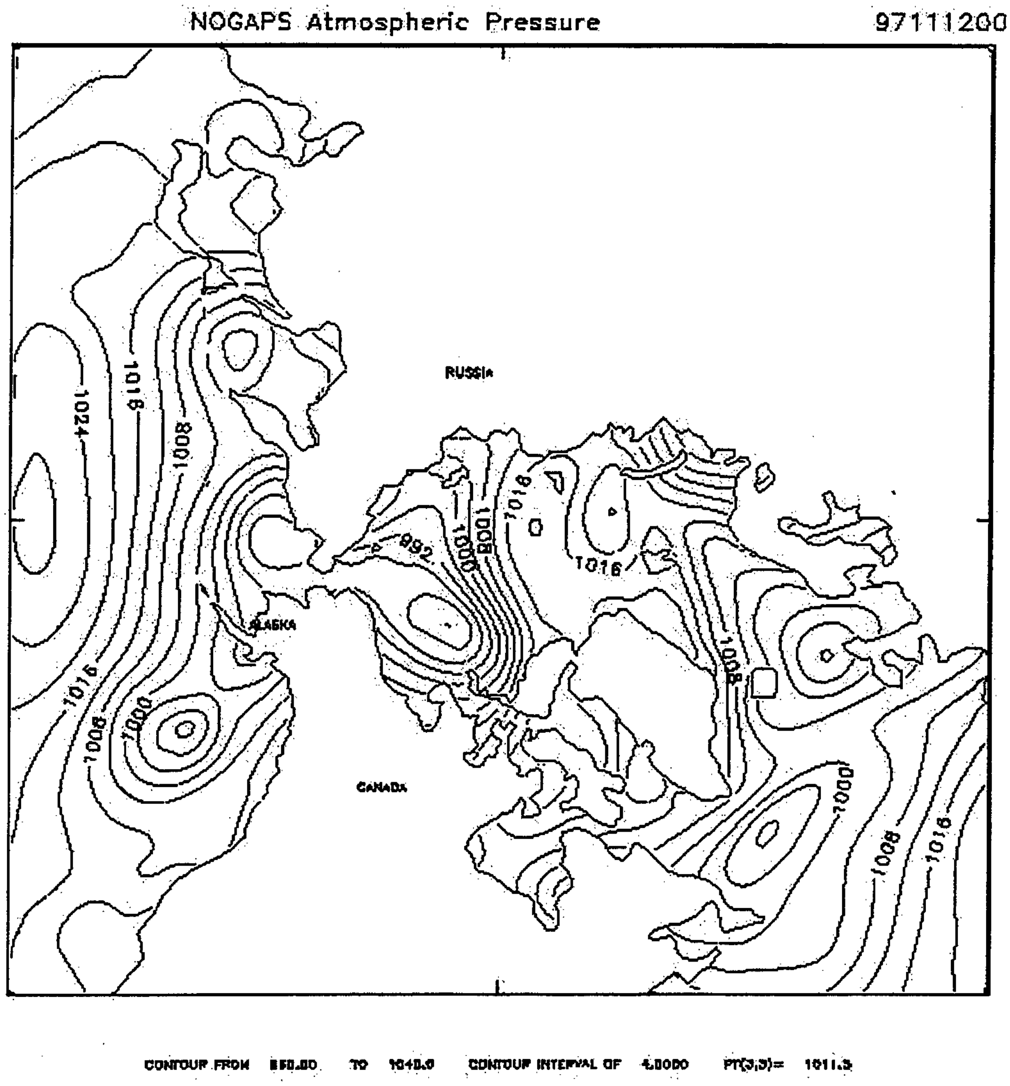

Figure 8. Atmospheric surface pressure during the mid-November ice drift direction reversal. The low pressure center, transiting the Beaufort Sea north of Alaska, caused a temporary reversal to the westward drift of the Beaufort Gyre in this area.

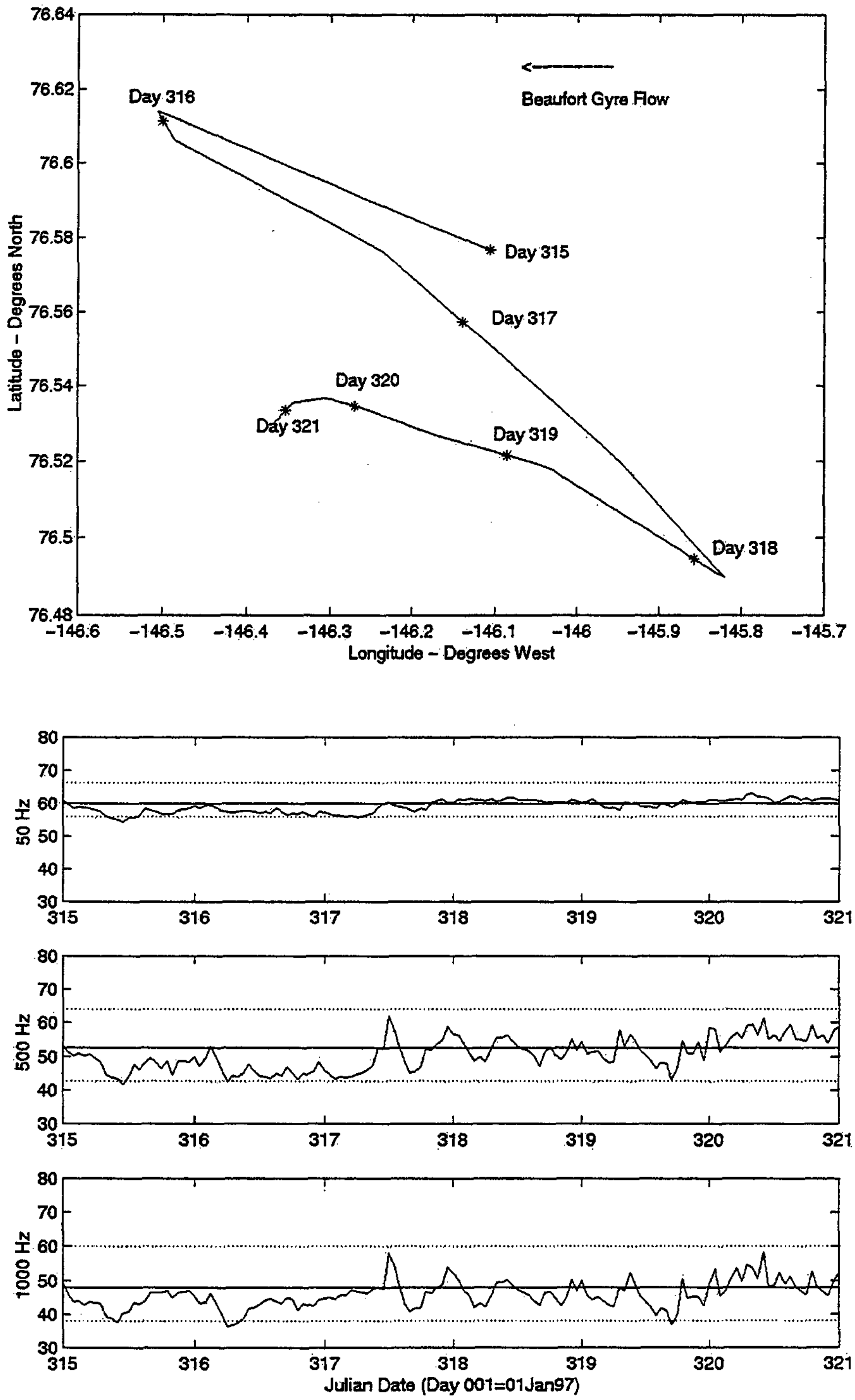

Figure 9. Drift track and noise record of the buoys during the mid-November drift direction reversal. The dotted lines on the noise record indicate the 95th and 5th percentile levels. Note that extremely high noise levels were recorded during periods of rapid direction changes (day 316 and 318).

that Leg 2 contained little local forcing and therefore, when compared with the other legs, lower noise production above 200 Hz.

Leg 3 (July-August 1998) occurred during a period of strong forcing due to an unusually strong and long lasting summer storm. The drift direction abruptly turned from northerly to east-southeast and tracked in a relatively straight line without much meandering as the wind forcing overpowered any inertial forcing. The storm produced the strongest mean winds (over 5 m/s) and therefore the highest mean ice speeds (12-13 cm/s) of the investigation, partly due to the extreme open nature of the ice during late July and August of 1998. The high leg displacement speeds (2-3 times higher than the other legs) of the buoys and ship are indicative of the nearly linear drift path in response to the strong and persistent wind forcing that occurred during the leg. Close examination of the stick plot (Figure 7) reveals the close association between the strong westerly winds and correspondingly high speed drift tracks to the east. The subsequent high-energy collisions of the ice during this 11 day event lead to elevated levels of high frequency noise. The 800 Hz median noise level peak for the summer occurred during Leg 3 for both buoys. The low frequency noise response was not as clear. The storm undoubtedly increased the noise levels, but the lack of meandering, eddy-like motions, leading to convergence of the ice as in Legs 2 and 4, served to limit low frequency noise production and obscured any increase in noise level due to the storm.

Leg 4 (August-September 1998) showed a clear contrast to the storminess of Leg 3. As high pressure built into the area, the Beaufort Gyre re-established itself and the ice flow returned to a northerly direction. All three drift tracks returned to the convoluted, eddy-like motion that preceded the storm of Leg 3 as wind forcing decreased and again allowed inertial motion to influence the ice direction. As expected, the ambient noise levels decreased from Leg 3 and returned to levels comparable with Leg 2.

IV. SYNOPTIC EVENT ANALYSIS

In previous studies, two different approaches were utilized to model low frequency ambient noise in the Arctic Ocean. Most efforts concentrated on characterizing the noise field in terms of local events and basing predictions on local environmental parameters (Dyer, 1988, Lewis and Denner, 1988). In general, this technique failed to produce an accurate Arctic noise model because basin-wide observations are now known to be necessary for accurate predictions. Studies today are now focused more on synoptic event analyses (Parsons, 1992, Feller, 1994) in order to identify environmental characteristics such as large-scale weather or ice motion that may be the cause of significant noise events.

A secondary goal of this research was to investigate two recently available environmental products to assess their utility towards improving ambient noise predictability: Radar Satellite Geophysical Processor System (RGPS) data and Polar Ice Prediction System (PIPS) energy dissipation data. Both of these data sets will be compared with the ambient noise data recorded during the SHEBA field experiment. This chapter will adopt the synoptic viewpoint in an effort to identify the relationship between the RGPS and PIPS products with notable events in the noise record. In order to identify and measure the significance of an ambient noise event, the 5th and 95th percentile levels, along with the median of the seasonal (summer or winter) noise level, are plotted on the ambient noise level time series that follow.

Four events were chosen for analysis. The first two events were high noise level events that occurred during the winter. The first event was associated with a distant noise source while the second was a locally generated event. The third event was a period of low noise level that took place in winter while the fourth was a series of high noise level episodes that occurred during late summer.

A. SYNOPTIC EVENT OF 29-30 OCTOBER 1997 (JULIAN DATE 302-303)

This event was chosen as an example of a loud noise event that propagated to the SHEBA site from a distant location, as indicated by the PIPS energy dissipation plot (Figure 10). A region of high-energy dissipation rate associated with storm-induced ice fracturing is observed along Ellesmere Island and the north Greenland coast. The high dissipation region extended northwest into the Beaufort Sea approximately 400-600 km from the hydrophones. At this time, the ice drift in the vicinity of the SHEBA camp appeared to be strongly influenced by the basin-wide flow of the Beaufort Gyre (the buoys and ship drifted linearly to the west-northwest) and did not appear to be responding to any local environmental forcing.

1. Description of the Noise Record

The 50 Hz and 500 Hz noise records are shown for Buoy 2 in Figure 11. The Buoy 1 record displayed a similar trend. Both frequencies showed a general increase in noise level during this two-day period, with the 50 Hz noise record demonstrating consistently high readings near the 95th percentile. In the Arctic, low frequency noise energy experiences much less transmission loss than high frequency noise energy (Urick, 1983). Since the noise-generating area was far from the local area, the low frequency noise levels recorded at the buoys were consistently high (near 95th

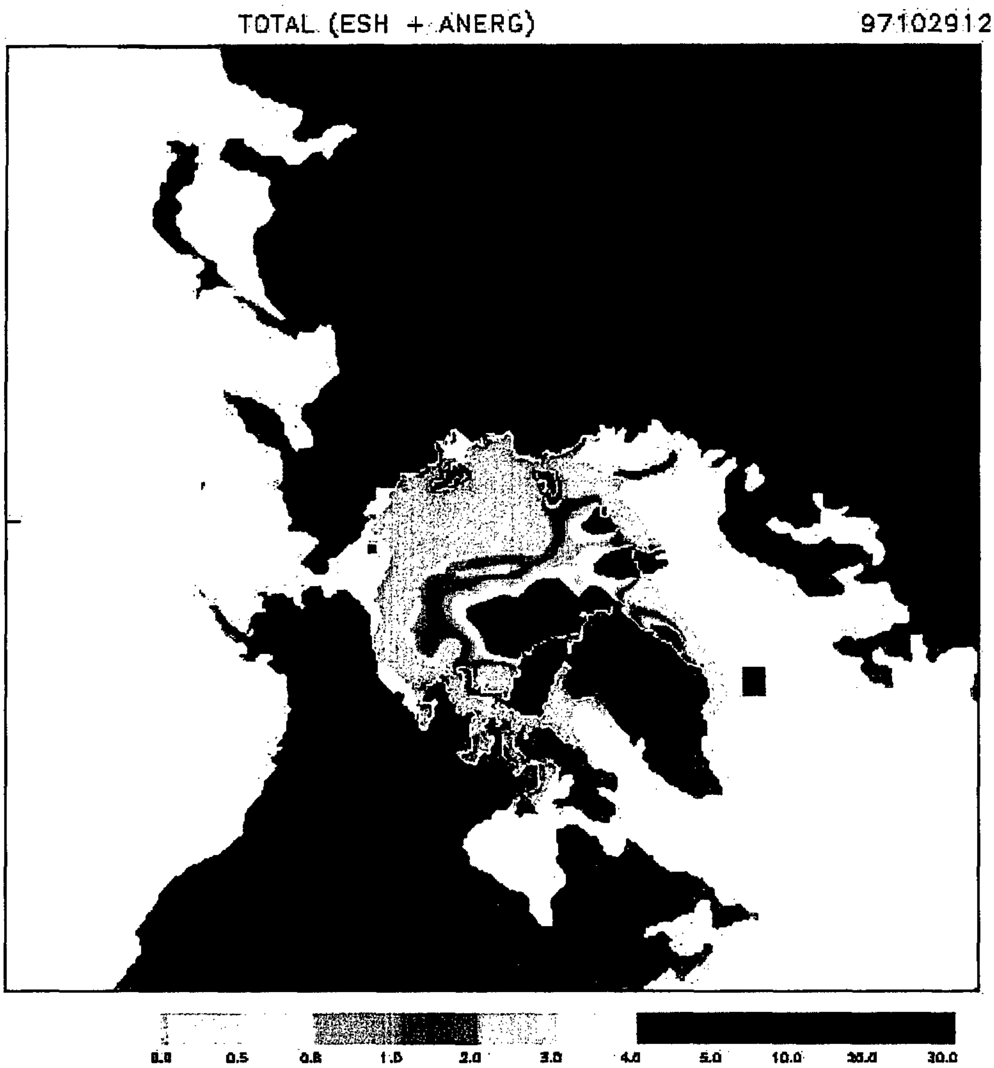

Figure 10. PIPS plot of energy dissipation rate measured in milli-Watts/m^2 during the distant noise event (29 Oct 97). Note the high energy dissipation rate extending from the Canadian Archipelago and Greenland into the central Arctic.

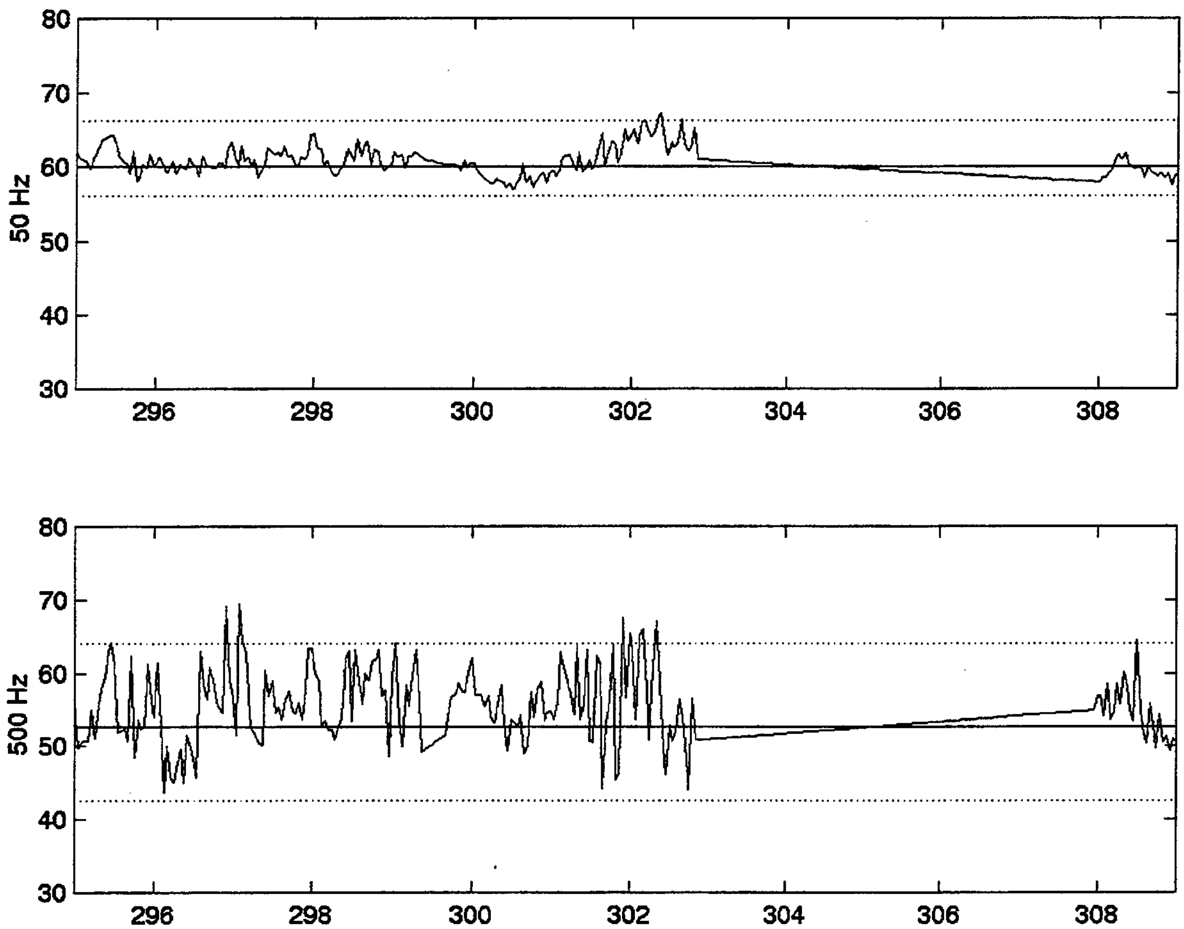

Figure 11. Time series of low (50 Hz) and high (500 Hz) frequency noise levels for the distant noise event on day 302 and 303. The dotted lines indicate the 95th and 5th percentile levels.

percentile). On 29 October (302) high frequency noise levels also reached the 95th percentile, but with much greater amplitude variations demonstrating a phase interference pattern of 2-4 hours duration. On 30 October (303) high frequency noise levels rapidly decreased below the median while low frequency levels remained high, indicating that the noise source was receding and demonstrating further evidence of the effect of transmission loss in the Arctic on the ambient noise spectrum.

2. Description of the RGPS Plot

The RGPS plot (Figure 12) for the period showed some areas of deformation of the ice to the west of the main SHEBA site. However, 50 km to the northeast of the main SHEBA site, near the area of the ambient noise buoys, deformation was sporadic, indicative of an absence of any organized forcing event. Clearly local ice deformation, as indicated by the RGPS plot, was not the cause of the high ambient noise levels recorded at the buoys during this time. The RGPS plot suggests that the source of the noise was beyond the range of the plot.

3. Description of the Energy Dissipation Rate Plot

The PIPS contours of energy dissipation rate due to fracturing of the icepack is presented in Figure 10. The plots for 29 and 30 October (302 and 303) are nearly identical, showing high levels of energy dissipation near the Canadian Archipelago and northern Greenland with broad areas of moderate (5-10 milli-Watts/m^2) energy dissipation extending well into the central Arctic. The coastal zones of the Canadian Archipelago and northern Greenland are a frequent region of high-energy dissipation

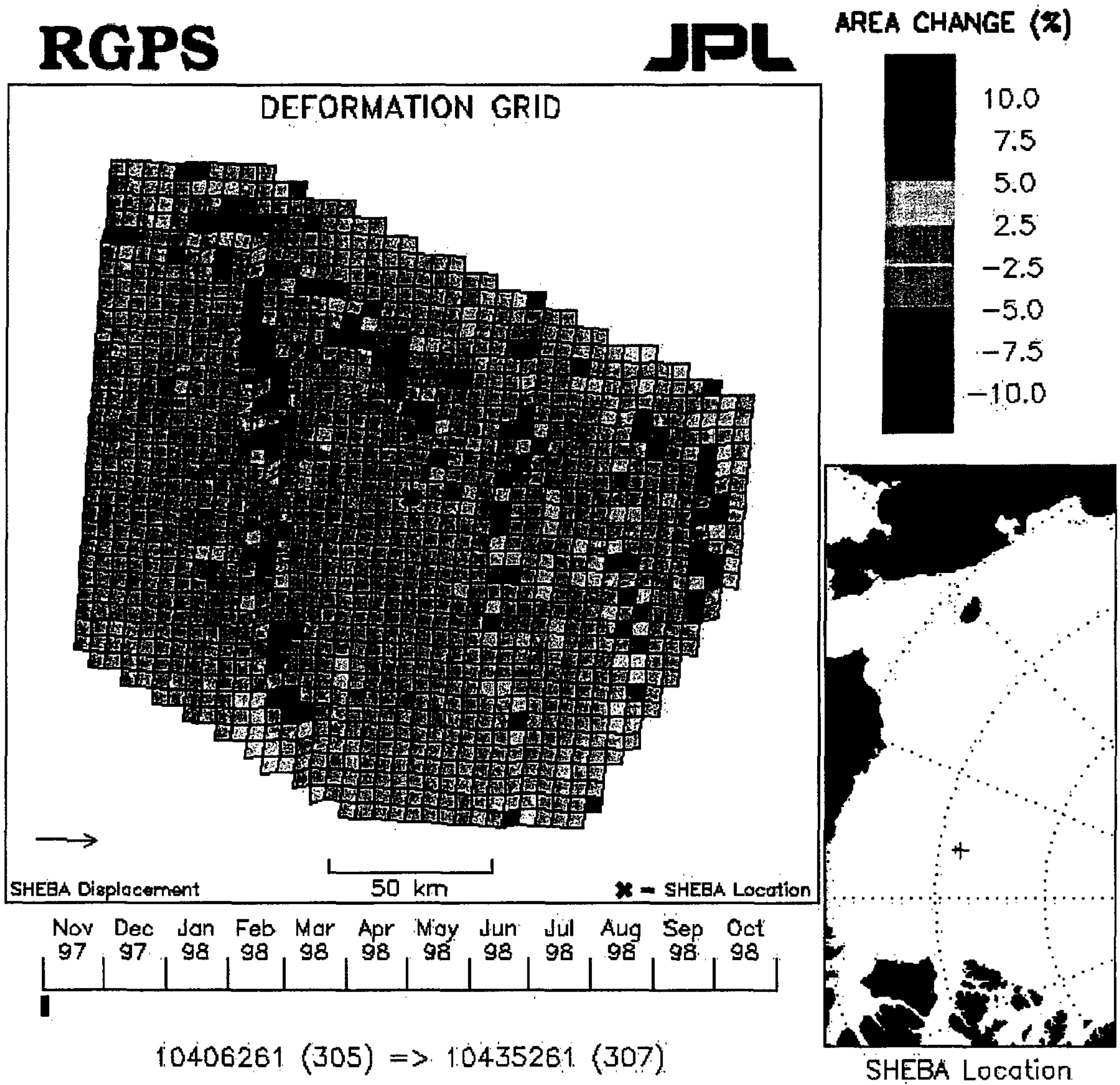

Figure 12. RGPS plot for 31 Oct 97 through 2 Nov 97 showing little local deformation present during the distant noise event.

due to the onshore direction of the ice drift in this area (Bourke and Garrett, 1987). When the ice convergence in this area becomes very intense, the energy dissipation begins to branch out across the Arctic Ocean, increasing levels throughout the central, deep-water areas. When the energy dissipation levels within 500 km of the SHEBA camp began to reach levels of 5-10 milli-Watts/m^2, the ambient noise levels at the SHEBA site also began to rise, as observed during this event.

4. Description of Environmental Factors

The atmospheric surface pressure chart for this time period (Figure 13) indicated an intense low-pressure center dominated the central Arctic near the pole. This strong cyclone was most likely responsible for strong forcing across the central Arctic, which subsequently

lead to increased onshore ice flow and high levels of ice convergence and energy dissipation near the Canadian Archipelago and Greenland. However, in the Beaufort Sea, a weak ridge of high pressure was present which produced fair weather in the SHEBA region. This was verified in the moderate wind speeds (average of 4 m/s) and ice drift speeds (approximately 10 cm/s as compared to the long-term mean ice drift speed of 9 cm/s for Leg 1). Once again, this indicates that the elevated ambient levels were in response to forcing outside of the local region during this period.

5. Summary

This two-day period in late October 1997 was an example of a distant noise source effecting the ambient noise record of the buoys. It was shown that the noise

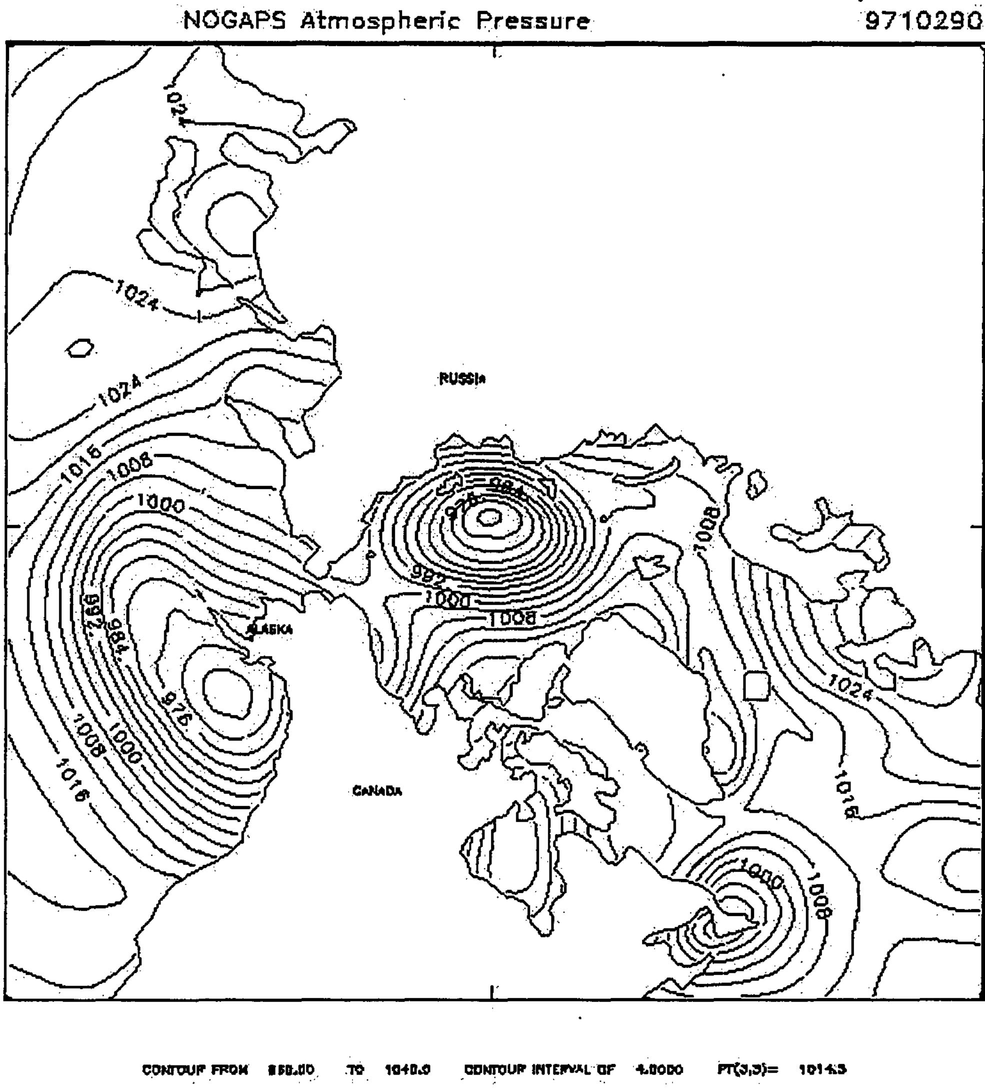

Figure 13. Atmospheric surface pressure during the distant noise event (29 Oct 97). A deep low pressure center near the pole resulted in a high degree of convergence near the Canadian Archipelago and Greenland. A weak high pressure ridge over the Beaufort Sea produced fair weather over the SHEBA region.

level at the buoys, particularly the low frequency noise level, was high in spite of little local energy dissipation, ice deformation, or environmental forcing. A powerful storm in the central-east Arctic served as a distant source of high noise energy. This was reflected in the energy dissipation plots and the behavior of the noise spectrum received at the buoys, both of which indicated that this scenario was a clear case of the effective potential for long distance noise propagation in the Arctic.

B. SYNOPTIC EVENT OF 5-7 DECEMBER 1997 (JULIAN DATA 339-341)

In contrast to the first synoptic event, this event demonstrated the effects of a local noise source on the ambient noise field. As anticipated, the presence of this local noise source was clearly reflected in all the observed environmental fields. The ice drift direction changed frequently as the floe experienced eddy-like motion and a reversal of the general direction of the mean flow (Figure 14).

1. Description of the Noise Record

Since Buoy 2 was inoperable during this time, Buoy 1's noise record was utilized. Unfortunately, as discussed in Chapter II, its high frequency data was corrupted, so only low frequency data (50 and 160 Hz) were used in this analysis. The noise record for this event (day 339-341) (Figure 15) is characterized by extremely high noise levels sustained near the 95th percentile with 3-9 hour long spikes registering well above the 95th percentile. As the noise source was located near the SHEBA region, the transmission loss was minimal and the measured noise level

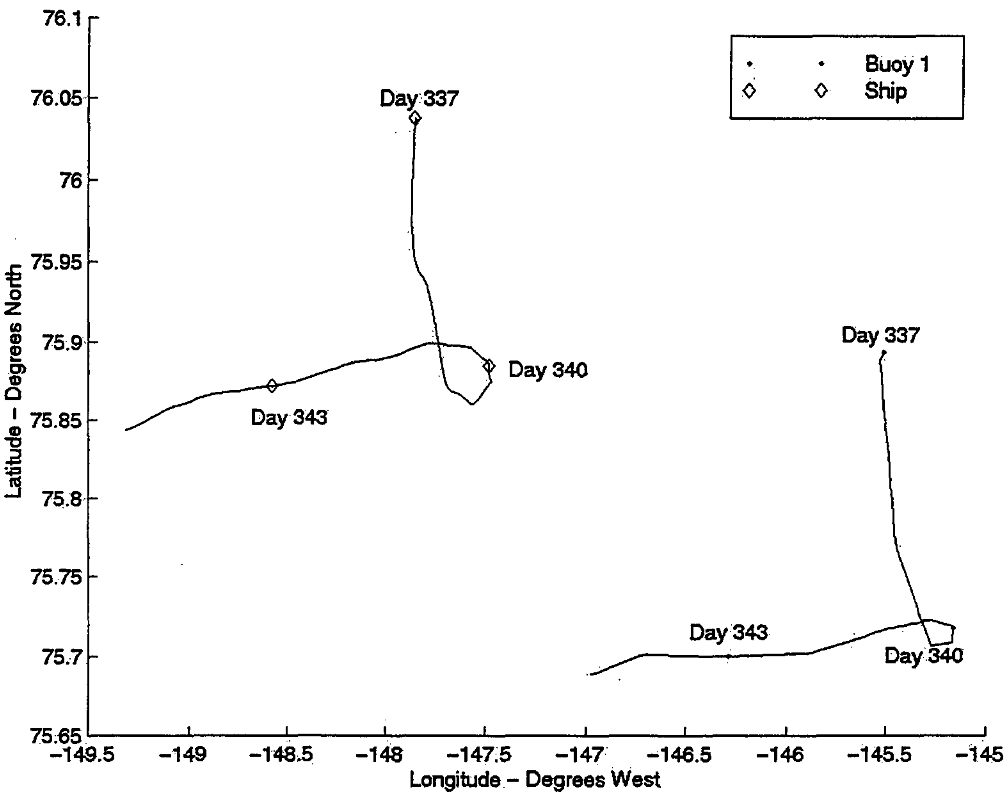

Figure 14. Ice drift plot during the local noise event, (4-6 Dec 97). The southerly leg of the drift was the result of forcing by a storm. As the storm left the region, the prevailing westward ice drift was re-established. The loop in the drift during the transition back to the prevailing drift direction resulted in strong convergence of the ice.

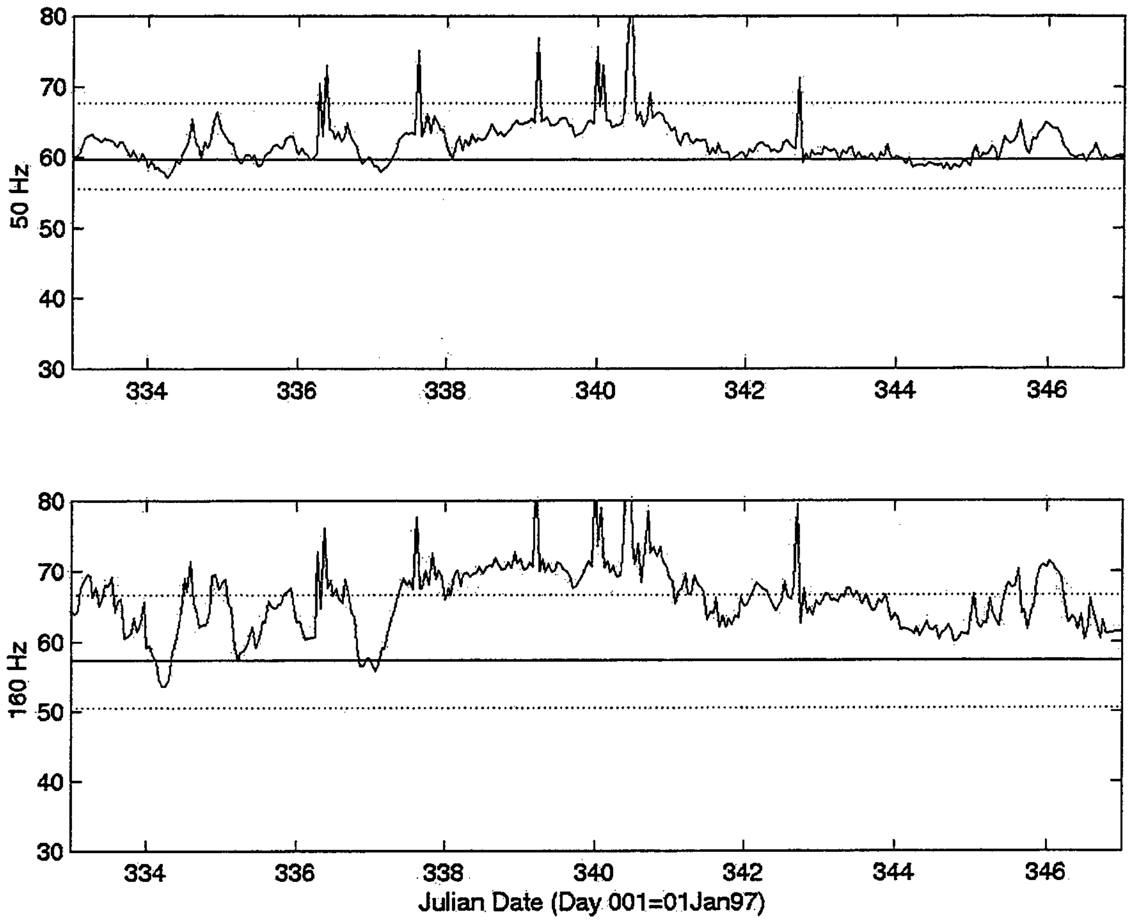

Figure 15. Time series of noise levels recorded during the local noise event (day 338-341). Dotted lines indicate 95th and 5th percentile levels. Note that the spikes near day 340 correspond to the loop in the ice drift identified in Figure 14.

was representative of the noise source level. Similar noise levels can be anticipated over the entire low frequency spectrum. This is evident as the noise level at 160 Hz was as high or greater than the noise levels at 50 Hz. The high noise level spikes, as much as 15 dB above the 95^{th} percentile, occurred simultaneously at both frequencies during a 24 hour period centered at 0000Z on 6 December (340). This is the same time that the ice drift track entered into an eddy-like loop (Figure 14). The rapid change in ice drift direction during this time, counter to the mean drift path, resulted in periods of strong convergence of the ice and subsequent ice fracture resulting in newly formed pressure ridges. Increased noise levels during convoluted, eddy-like motion leading to strong convergence of the floe field has been noted in other ambient noise investigations in the Arctic (Bourke and Feller, 1999).

2. Description of the RGPS Plot

The deformation of the ice near the SHEBA site, indicated by the RGPS plot, is shown in Figure 16. Buoy 1 was 40 km to the southeast of the ship during this time, near a large, organized seam of ice convergence and deformation. This area of activity south of SHEBA was most likely a direct result of the rapid direction changes and eddy-like motion of the ice drift and seemed to have been the source of the high ambient noise.

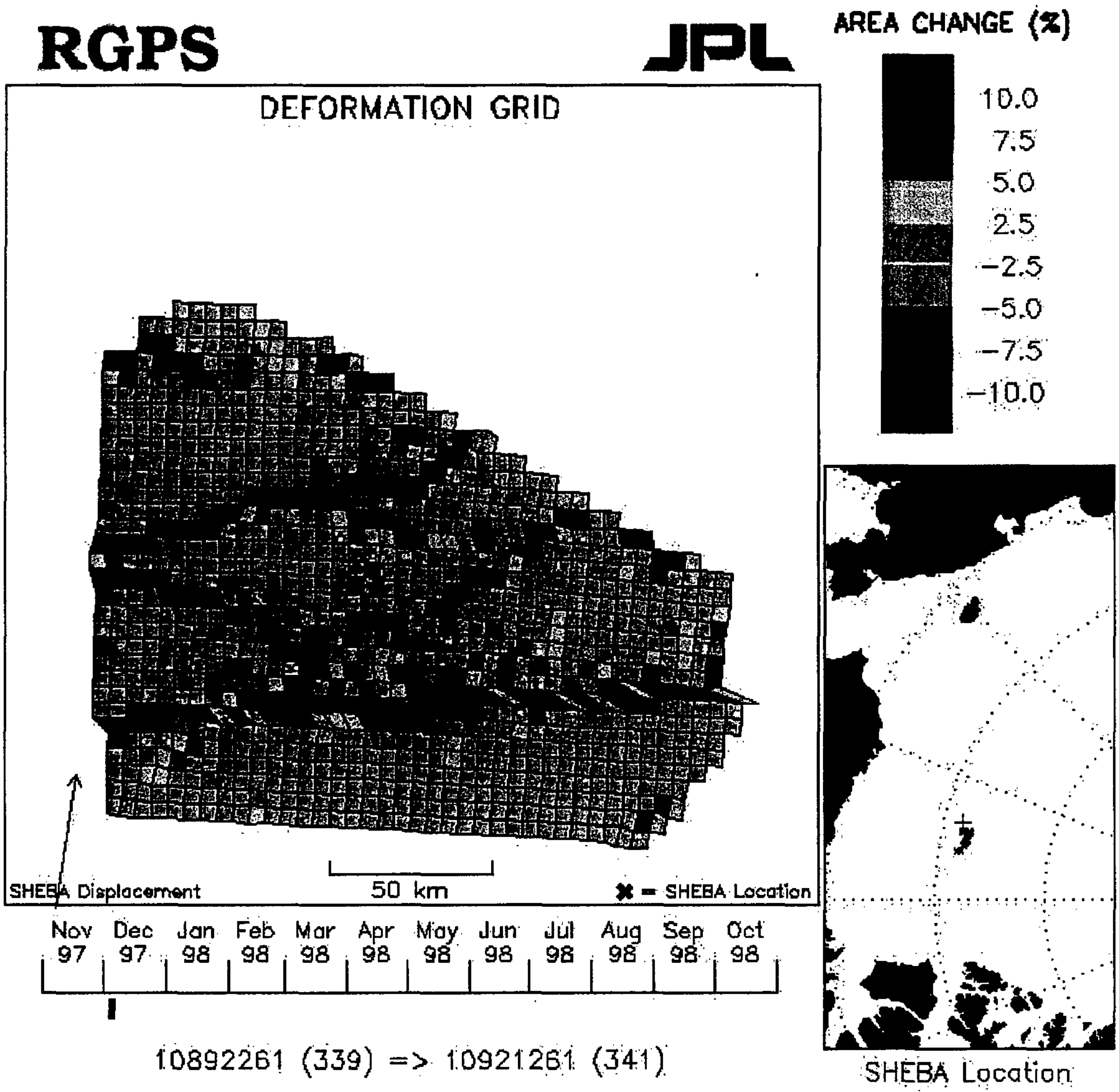

Figure 16. RGPS plot for 4-5 Dec 97 during the local noise event. Note high levels of deformation to the south of the SHEBA camp.

3. Description of the Energy Dissipation Plot (Pips Output)

The energy dissipation plot shows an area of high-energy dissipation (near 10 milli-Watts/m^2) across the region of the SHEBA experiment (Figure 17). This is reflective of a high degree of forcing being applied to the ice and the subsequent transfer of high levels of energy to the icepack in this area. Therefore, in this instance, the energy dissipation seems to be well correlated with the high levels of ambient noise.

4. Description of Environmental Factors

The atmospheric surface pressure chart for this time (Figure 18) depicts a trough of low pressure which extended into the Beaufort Sea from the semi-permanent Aleutian low pressure center located just south of the Bering Strait. The development of the trough resulted in a distinct wind shift across the SHEBA region. The prevailing east-northeasterly winds shifted to northwesterly on 1 December (335) and then veered back to northeasterly on 5 December (339). The ice drift reflected this wind change with convoluted, non-linear motions. The southerly track (Figure 14) of the ice drift from 3 December (337) until 5 December (339) was indicative of the forcing from the developing low pressure trough, while the eddy-like motion from 5 December (339) through 7 December (341) was the result of the wind reverting back to the prevailing east-northeast direction. As discussed earlier, rapid (1-2 day) changes in ice drift direction resulted in strong convergence of the ice field, which increased the ambient noise. High wind speeds (approximately 9 m/s) during

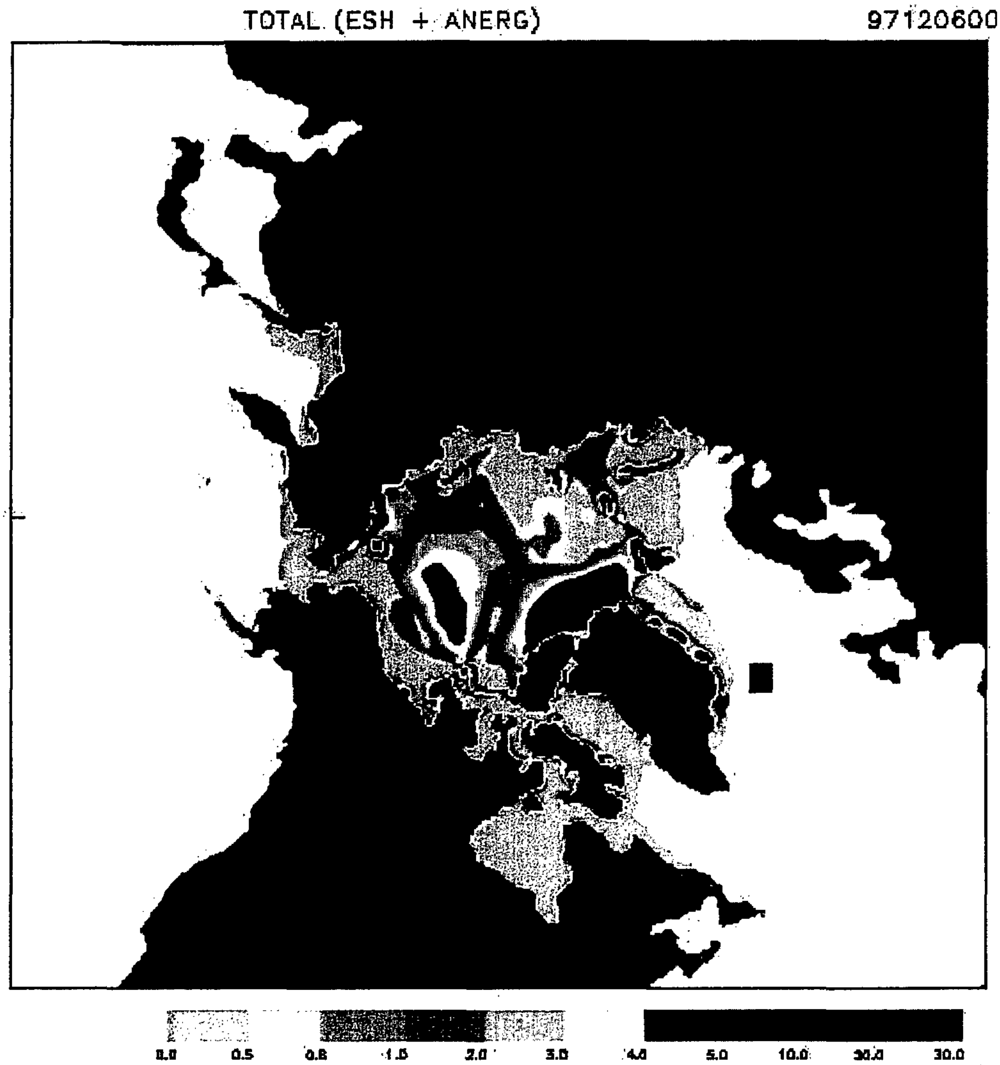

Figure 17. PIPS plot of energy dissipation rate measured in milli-Watts/m^2 for day 341 during the local noise event. Note high rates of energy dissipation across the SHEBA region.

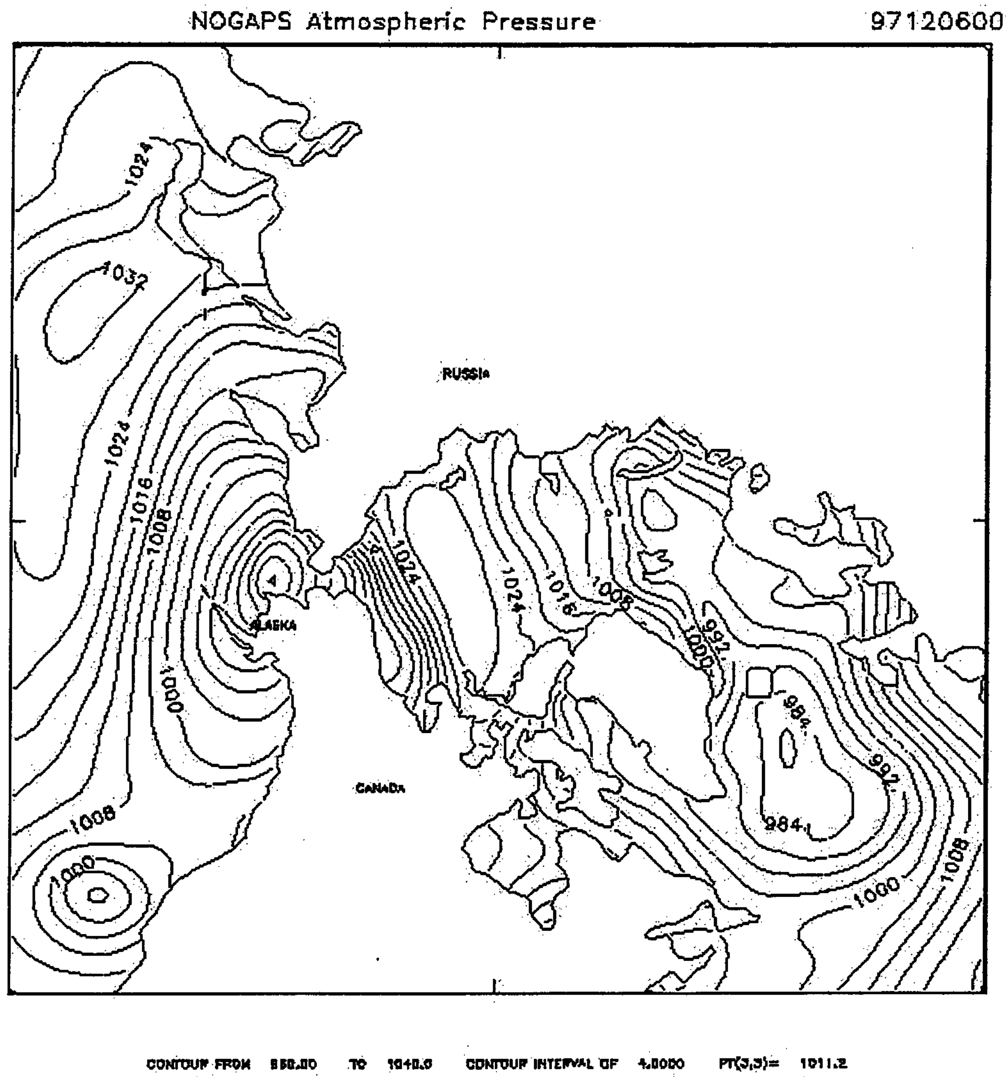

Figure 18. Atmospheric surface pressure during the local noise event (6 Dec 97). Note the high pressure gradient between a low pressure center near the Bering Strait and the broad area of high pressure over the pole. The strong gradient produced high wind speeds at the SHEBA camp.

this period served to increase the convergence by transferring energy to the ice drift and producing above-average ice speeds (15 cm/s as compared to the Leg 1 average of 9 cm/s).

5. Summary

This period in early December was a clear example of the effects of a nearby source of ambient noise. A developing trough, which extended into the Beaufort Sea from the south, resulted in a shift in the wind direction while increasing the wind intensity. As ice drift is predominantly wind-driven, this four-day perturbation in the prevailing wind direction caused a series of eddy-like motions that lead to the convergence and deformation of the ice and to locally high levels of energy dissipation that culminated in the high levels of ambient noise recorded at the buoys. These high levels, produced by local noise sources, were the highest recorded during the SHEBA experiment.

C. SYNOPTIC EVENT OF 4-5 NOVEMBER 1997 (JULIAN DATE 308-309)

This event provides an example of a quiet period during the generally noisy winter ambient noise record. In contrast to the local noise event of the previous section, where noise levels were as high as 83 dB at 50 Hz, this quiet event registered noise levels as low as 55 dB. During the winter, extended periods of low ambient noise are not rare, but are short lived as indicated by the median of the noise record, which was centered evenly between the 5^{th} and 95^{th} percentile at 60 dB. This suggests that the winter noise field is generally loud with intermittent, short-term periods of low or extremely high noise levels. This is in contrast to the summer situation when the opposite is true. In the Beaufort Sea the summer median noise level was much closer (within 5 dB) to the 5^{th} percentile than to the 95^{th} (15-20 dB). This implies that the summer noise field, in contrast to that of winter, is characterized by long periods of low ambient noise (approximately 55 dB) punctuated by short duration, high noise events, which can reach levels of up to 85 dB.

As a contrast to the other winter scenarios, this event emphasizes the lack of any forcing or noise source and the subsequent quiescent response of the noise field. During this period, the buoys drifted in a generally linear, west-northwest direction.

1. Description of the Noise Record

The ambient noise record during this quiet period is presented in Figure 19. The noise records during this period were characterized by frequency level as high frequencies responded to local, isolated noise sources that did not contribute as significantly to the low frequency noise levels. This resulted in less consistency in the high frequency noise field. The low frequency (50 Hz) plot was consistently less than the median while the higher frequency (500 and 1000 Hz) levels initially recorded moderate noise levels slightly higher than the median on 4 November (308) before declining below the median on 5 November (309). By 6 November (310), noise levels had risen back above the median at all frequencies.

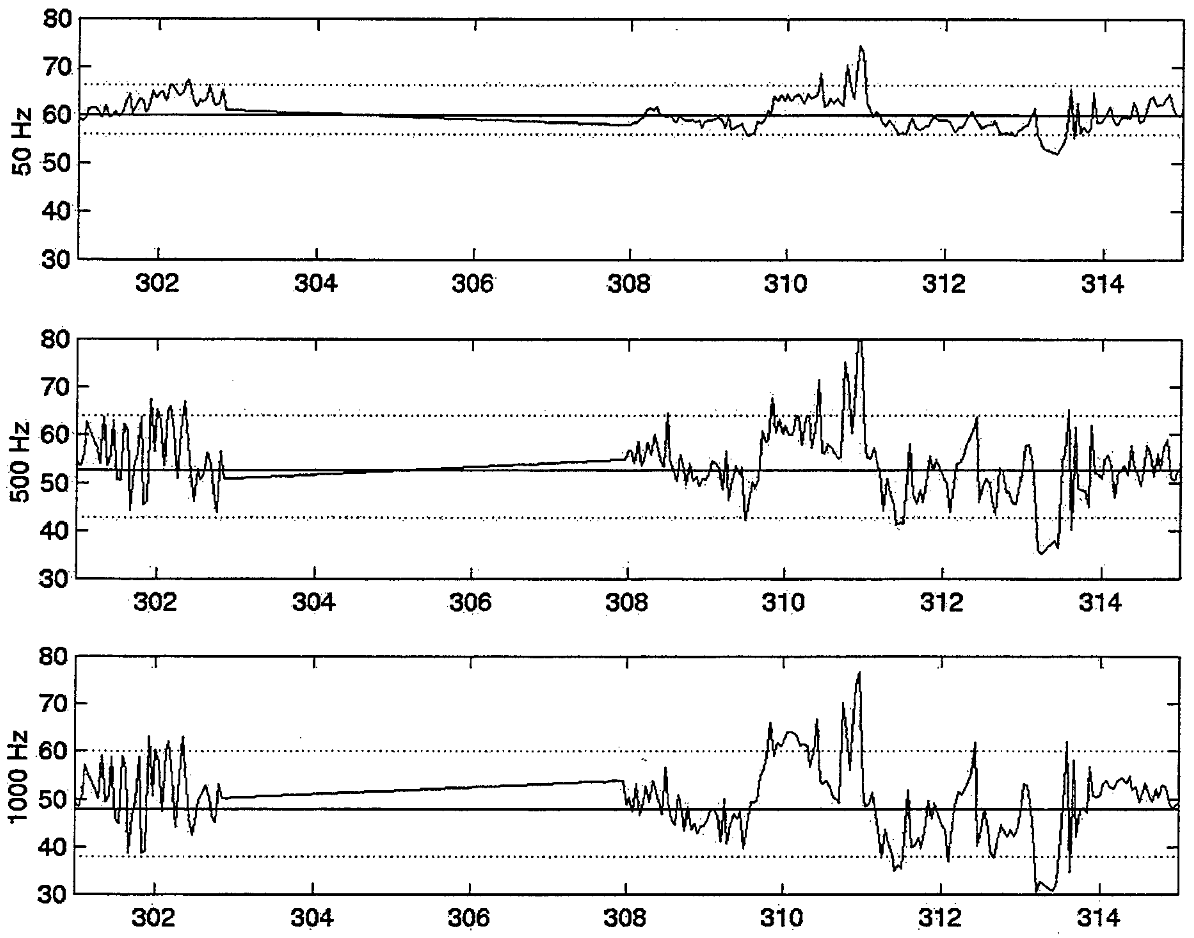

Figure 19. Time series of noise levels for three frequencies during the quiet noise event, which lasted from day 308 until day 310. The dotted lines indicate 95th and 5th percentile levels.

2. Description of the RGPS Plot

The RGPS plot (Figure 20) shows some deformation to the west of the SHEBA site, but very little near the location of the ambient noise buoys (north and east of SHEBA). The distribution of deformation in relation to the SHEBA site was consistent with the ambient noise record. During this period the buoys and ship drifted west and it appeared that deformation was increasing towards the west, which would explain the increased noise levels at the end of this quiet period.

3. Description of the Energy Dissipation Plot (Pips Output)

Energy dissipation was low across the entire Arctic basin during this time period, as indicated by Figure 21. There were some higher level readings (>5 milli-Watts/m^2) in the eastern Arctic near the north shores of Greenland and Svalbard, but the Beaufort Sea contained relatively low readings (0.5-1 milli-Watts/m^2). The tongue of high energy dissipation levels that in winter usually extends from the high convergence area along the north shore of the Canadian Archipelago and Greenland into the Beaufort Sea was relatively weak during this period as compared to the distant noise source event depicted in Figure 10.

4. Description of Environmental Factors

The surface atmospheric pressure chart (Figure 22) for 4 November (308) shows that a high-pressure ridge dominated the Arctic, particularly the Beaufort Sea region, during this time. This type of meteorological regime produced the light winds

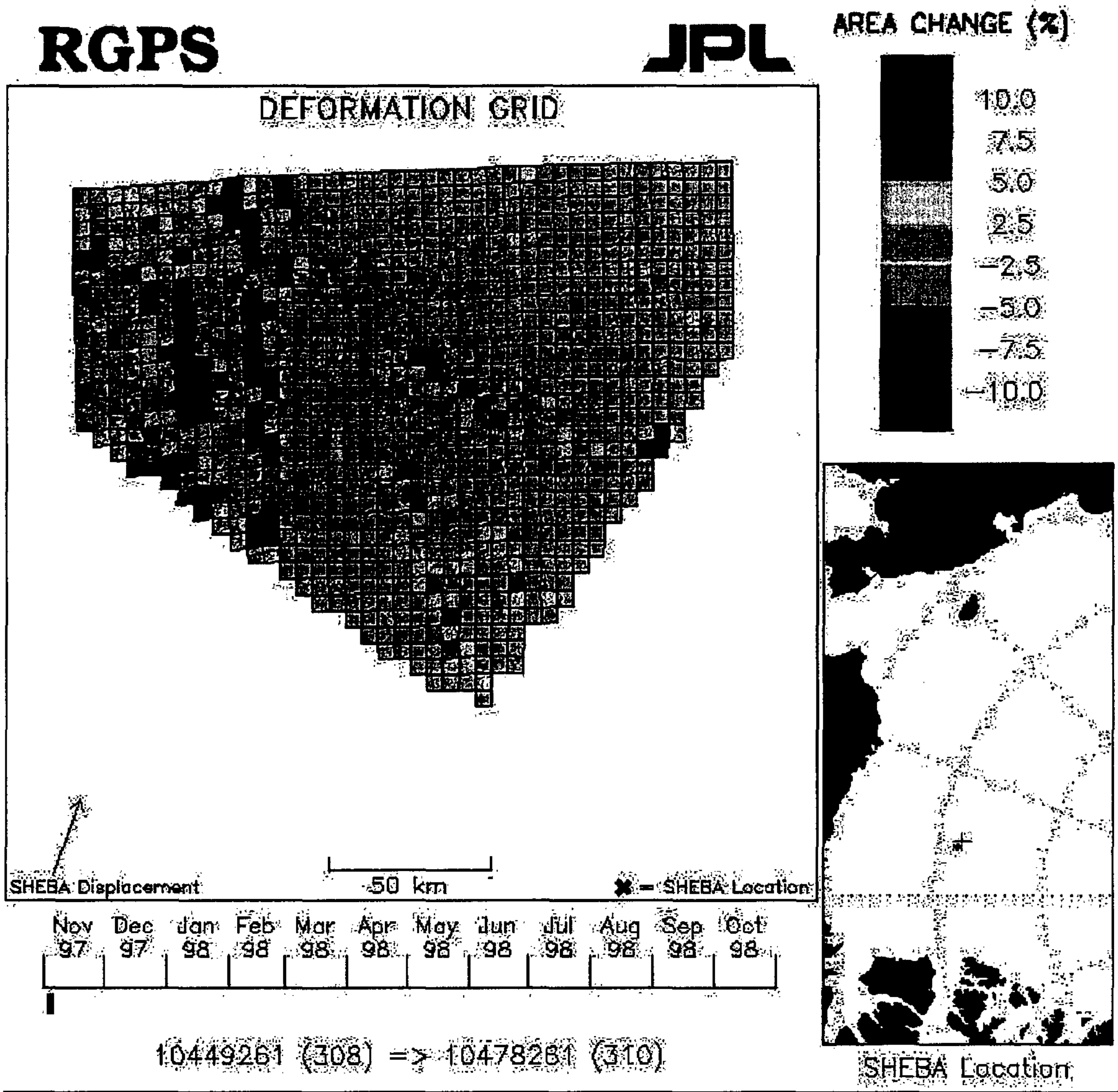

Figure 20. RGPS plot for 3-5 Nov 97 during the quiet noise event. Note low levels of deformation in the local SHEBA area.

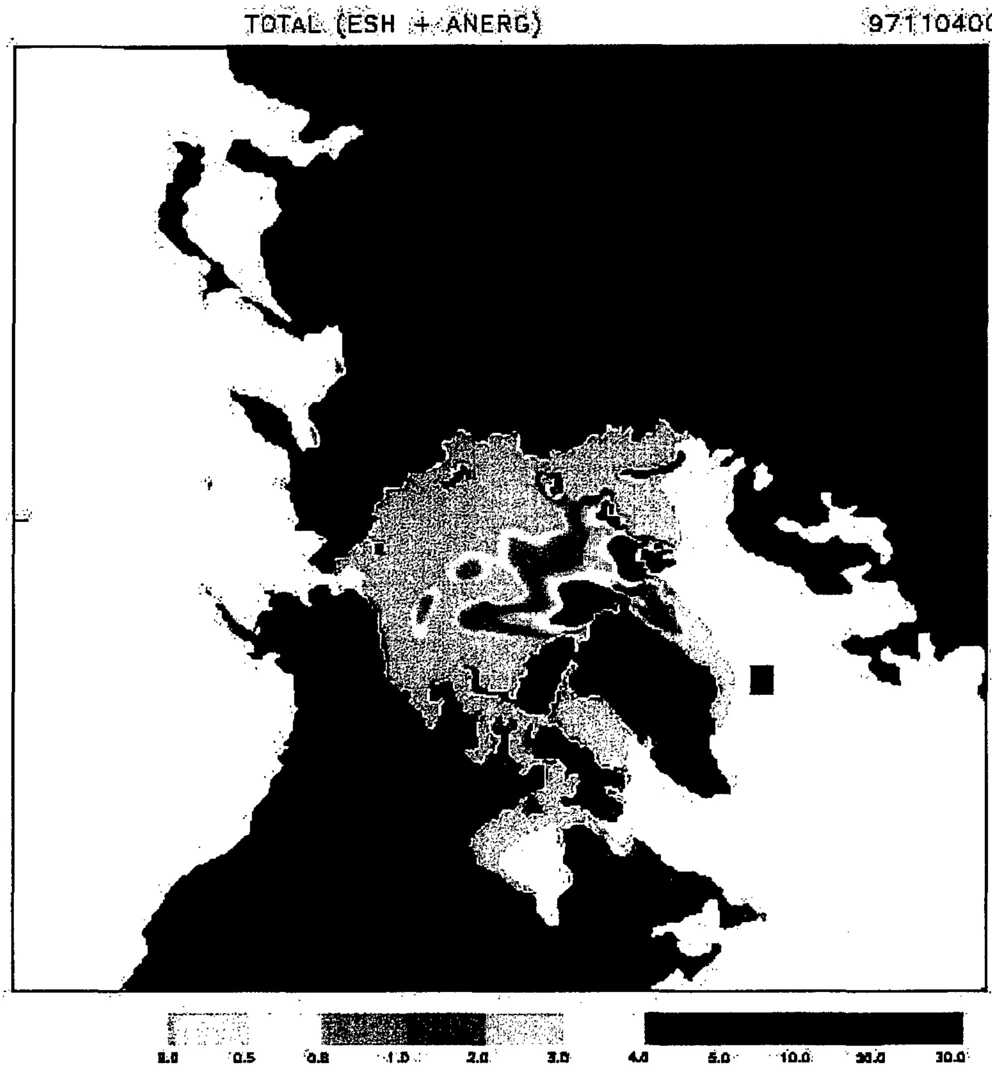

Figure 21. PIPS plot of energy dissipation rate measured in milli-Watts/m^2 for 4 Nov 97 during the quiet noise event. Note the lack of energy dissipation in the western Arctic and the retreat of high levels to the extreme east Arctic.

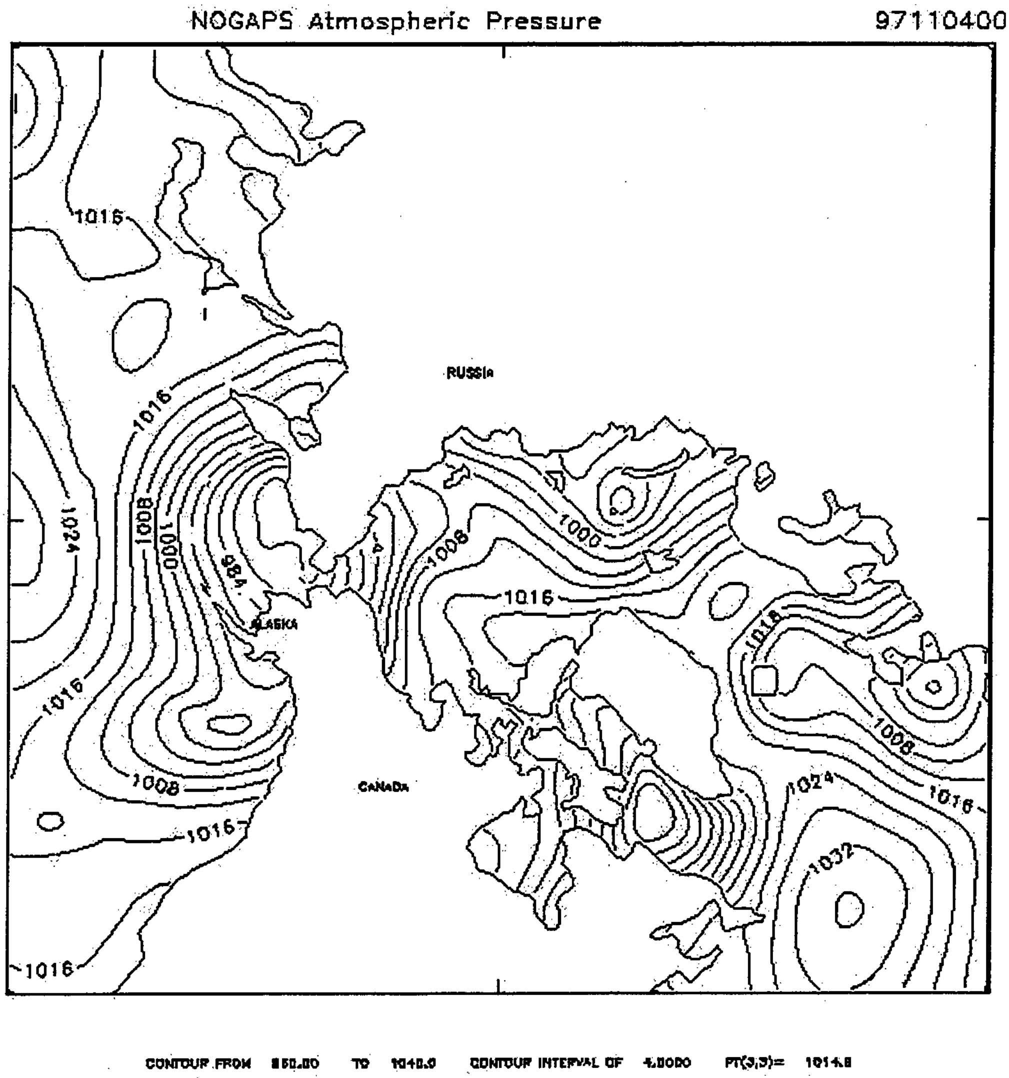

Figure 22. Atmospheric surface pressure chart during the quiet noise event (4 Nov 97). High pressure dominated the Arctic with minimal pressure gradient over the SHEBA area.

(3 m/s) and slow drift speeds (10 cm/s as compared to the Leg 1 average of 9 cm/s), observed during this event.

By 6 November (310), a trough developed from a low-pressure center in the Bering Sea and extended into the Beaufort Sea. The arrival of the low-pressure trough and its associated higher wind speeds was most likely responsible for ending this two-day period of low ambient noise.

5. Summary

This event was analyzed in order to illustrate the conditions that can lead to a period of low ambient noise even during the noisy winter period. Fair weather is an important factor to consider when forecasting low levels of ambient noise, but basin-wide low energy dissipation (i.e., absence of distant storms) and a lack of local deformation must accompany it. As demonstrated in the first event, distant noise sources can exert a noticeable effect on ambient noise levels measured at remote sites. Therefore, in order to identify quiet ambient noise events, one must consider the environmental factors across an entire region, rather than just local conditions.

D. HIGH AMBIENT NOISE EVENT DURING SUMMER ICE CONDITIONS 7-22 AUGUST 1998 (JULIAN DATE 585-600)

During the Arctic summer, ice conditions are radically different from that observed in winter. Melting ice and constant solar energy input lead to more open water. The fractured ice floes are able to reach much higher drift speeds and move more independently than during the winter when the icepack is nearly contiguous.

This has a notable effect on the ambient noise level. As mentioned in the previous section, the summer noise field is characterized by long periods of relatively low ambient noise, which occur when the separate ice floes are drifting in a common direction with few perturbations. When forcing is applied, such as during a storm, changes in drift direction produce high-energy ice-ice collisions, which produce noise levels up to 25 dB greater than the median of the summer noise record.

As discussed in Chapter I, the summer of 1998 was unique as the Marginal Ice Zone (MIZ) reached much farther north and the ice was more open than in past years. During the two-week period from 7 August (585) until 22 August (600), there were several high ambient noise events of which two will be examined in light of summer ice conditions.

1. Description of the Noise Record

The ambient noise level during this period was characterized by occasional high-level noise events, which punctuated an otherwise relatively quiet period. The ambient noise levels of the two buoys are shown for a low (50 Hz) and a high (500 Hz) frequency in Figure 23. The noise records of the two buoys appear highly correlated, with high noise events occurring on 7 August (585), 12 August (590), 15 August (593), and 19 August (597). The 12 August (590) and 19 August (597) events were chosen for analysis, as these events were consistently reflected in the noise record of the buoys.

The 12 August (590) event was discernable in the noise data of both buoys except for the high frequency data of Buoy 2, a fluctuation most likely due to the local

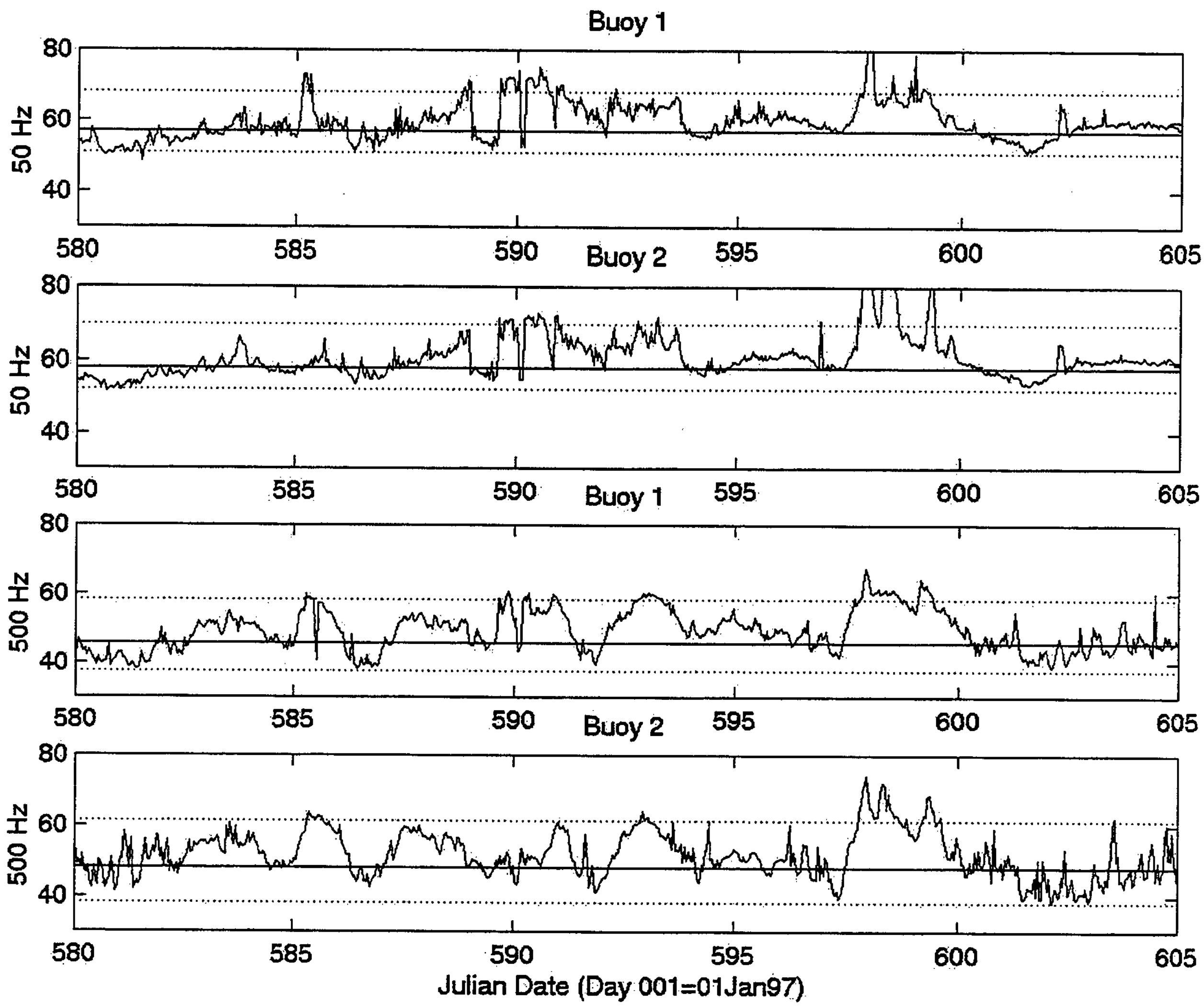

Figure 23. Time series of low (50 Hz) and high (500 Hz) noise levels for both buoys during the summer high noise events (day 587-600). Dotted lines indicate 95th and 5th percentile levels.

nature of high frequency noise. It is possible that in the immediate vicinity of Buoy 2 there may have been less activity than the rest of the overall region, which would have resulted in lower high frequency noise levels whereas the 50 Hz noise levels were influenced by noise propagating from distant sources.

Buoy 1 recorded ambient noise levels near the summertime 95th percentile at both high and low frequencies during the 12 August (590) event. Although the noise levels occasionally dropped to near the median level during this event, and therefore did not have the consistency of the continually high levels experienced in winter, both buoys did record noise peaks near the 95th percentile mark for a period of 1-2 days.

On 19 August (597), both buoys experienced extremely high noise levels at all frequencies. Noise levels were recorded well above the 95th percentile and remained steadily high for a period of approximately two days. This event appears to have been more energetic, consistent, and widespread than the 12 August (590) event.

2. Description of the RGPS Plot

The RGPS plots (Figures 24 and 25) show a great deal of deformation, a feature observed in nearly all the RGPS plots during the summer period. Throughout the summer, a high degree of deformation was observed, even during periods of low ambient noise. This is due to the unconsolidated, open nature of the pack ice. At this time of year, the icepack consisted of many individual floes (Figure 4), each moving independently. Since RGPS compares the differences in the observations of a gridded area over intervals of 1-3 days, it most accurately portrays pressure ridge activity when the grid is generally stationary and coherent during the consolidated ice

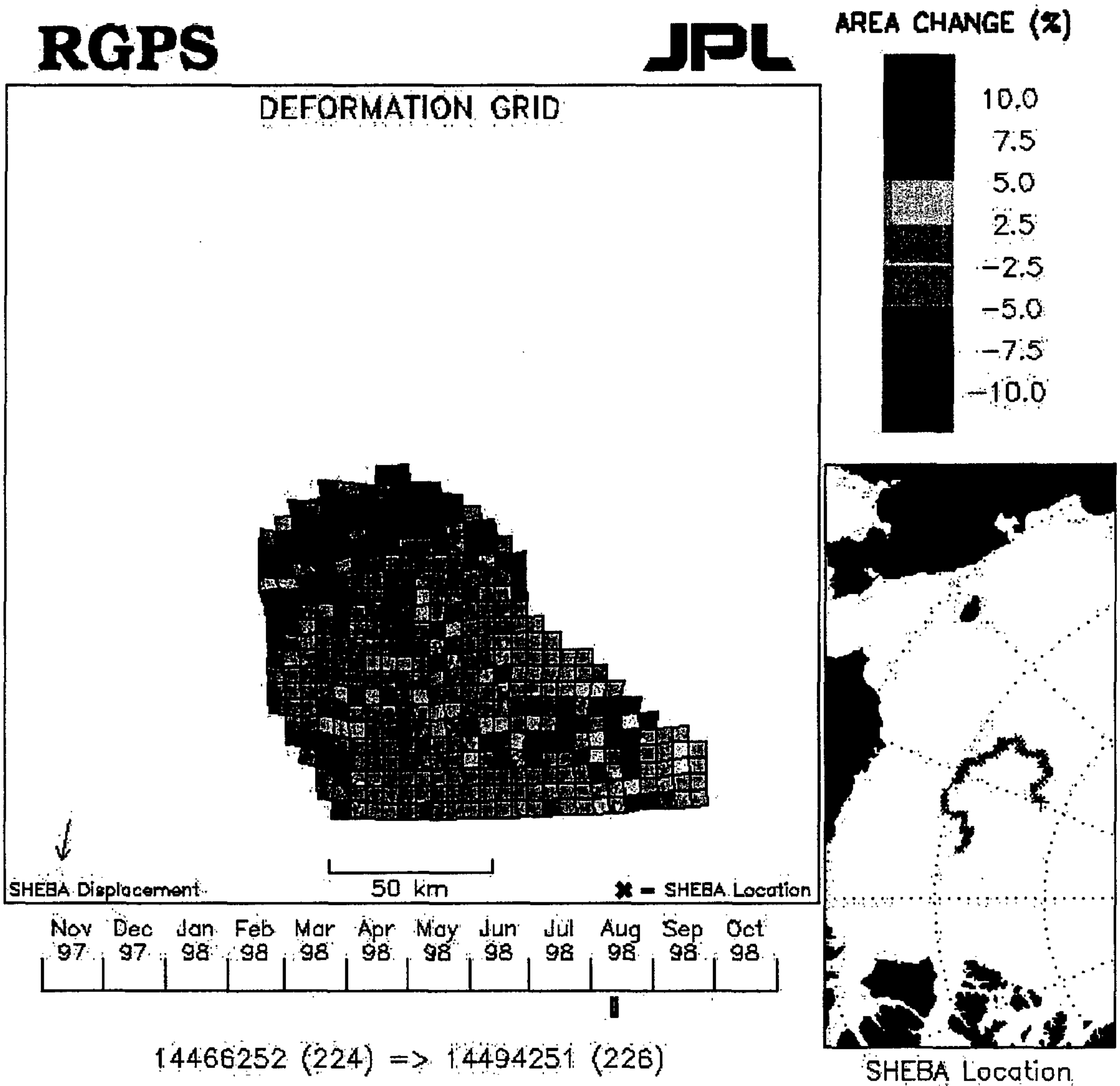

Figure 24. RGPS plot for the first summer high noise event (day 589-591).

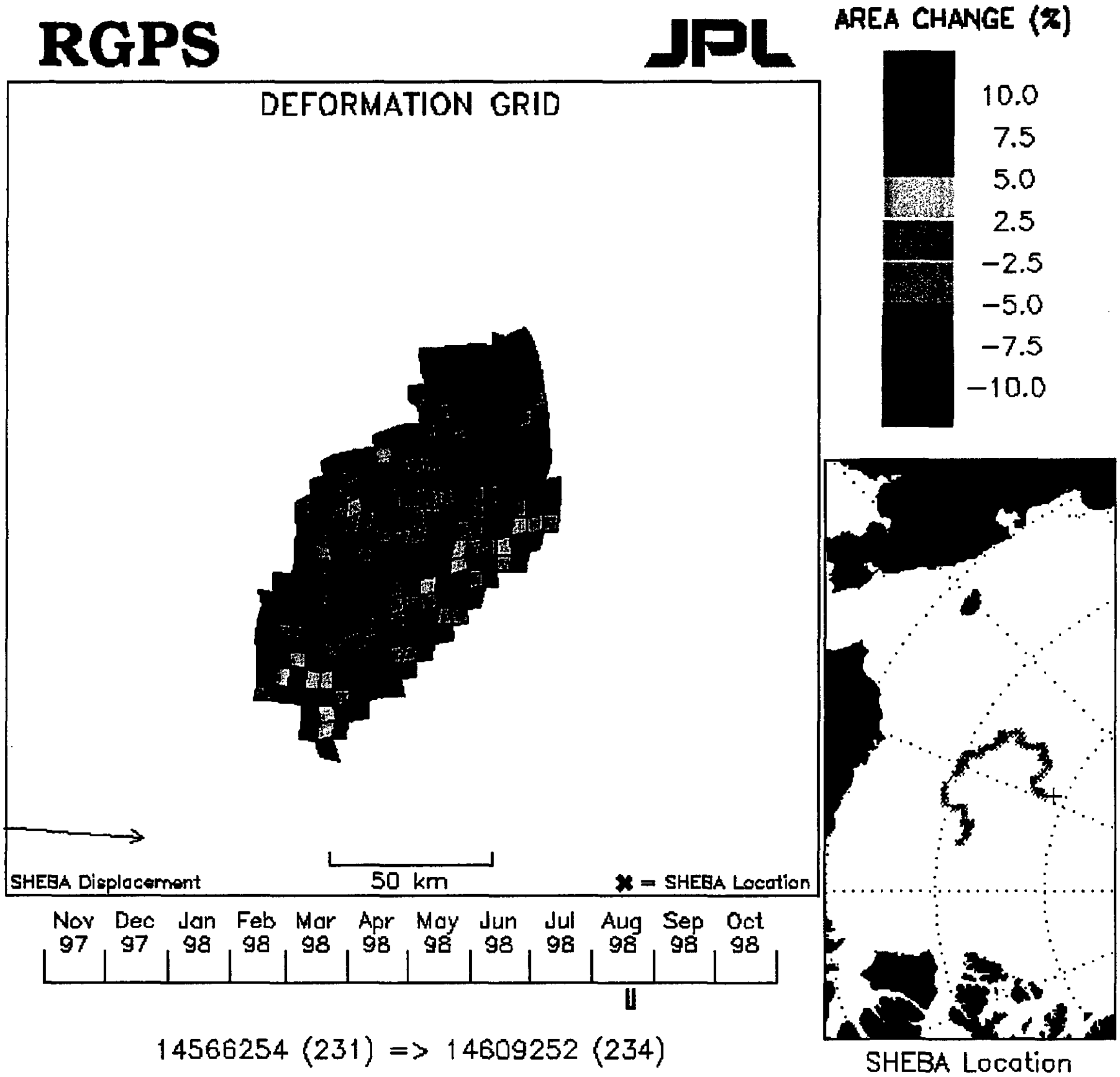

Figure 25. RGPS plot for the second summer high noise event (day 596-599).

conditions of winter. This allows areas of motion (divergence or convergence) to be clearly identified. During the summer, however, the entire grid is deformed as multiple ice floes move independently of one another. Therefore, during the summer, the high degree of deformation depicted in the RGPS plots were not accurately correlated with high noise levels.

3. Description of the Energy Dissipation Plot (Pips Output)

PIPS was also ineffectual in identifying areas of high ambient noise. As the summer ice pack was in free drift, internal stress was essentially zero, which was indicated by a lack of energy dissipation on the PIPS plot (Figure 26) during the period. Energy dissipation continued to be very low throughout the summer-long free drift. This implies that the majority of the ambient noise generated during the summer was caused by high-energy collisions during summer cyclonic storms.

4. Description of Environmental Factors

The surface atmospheric pressure charts for the two events (Figure 27 and 28 for 12 and 19 August, respectively) both indicated that a trough of low pressure extended into the Beaufort Sea from a low pressure center near the Bering Strait. On 12 August (590) the trough was fairly weak, but still induced a significant wind direction change. Winds were prevailing from the south before the event, but shifted to northerly and increased to 6-8 m/s from 12-17 August (590-595) before returning to southerly. This rapid change in wind direction resulted in the convoluted, eddy-

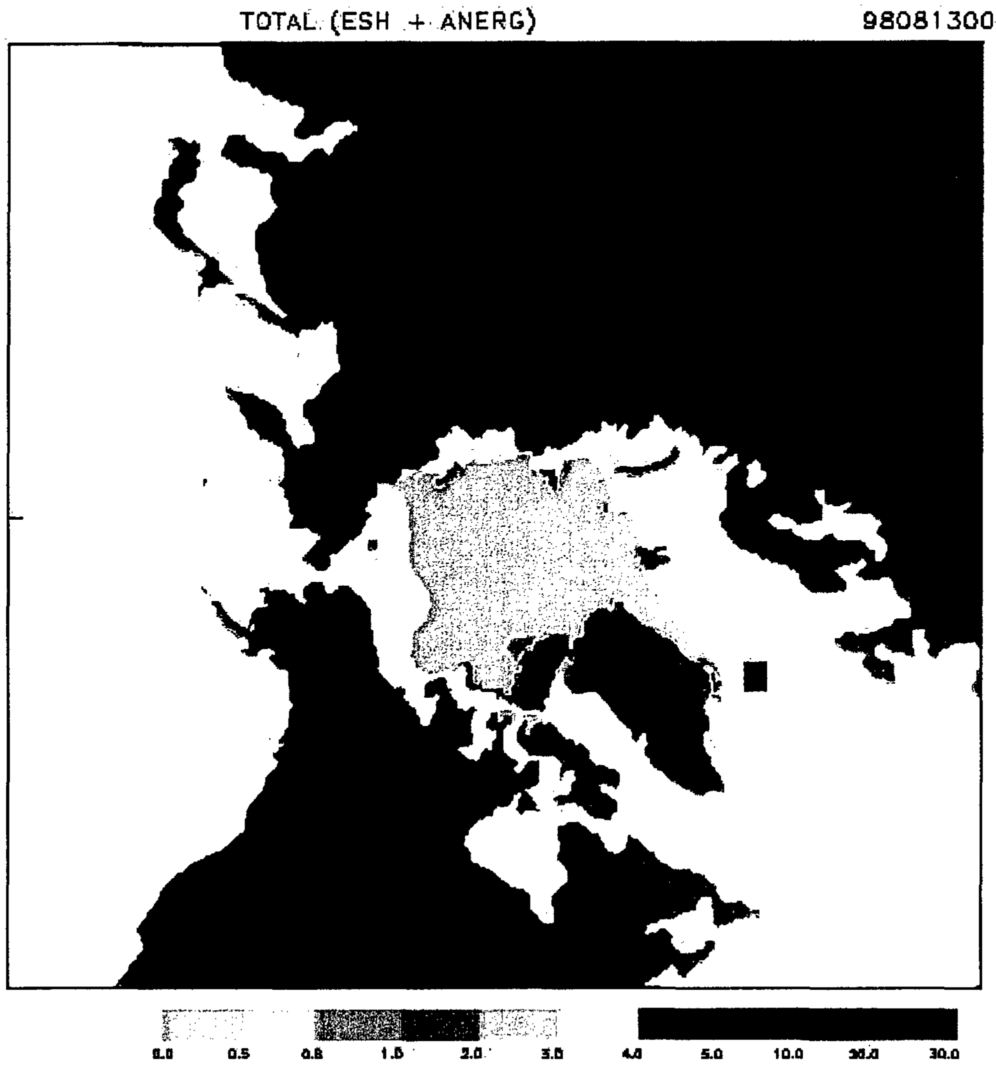

Figure 26. PIPS plot of energy dissipation rate measured in milli-Watts/m^2 for the first summer noise event (day 591).

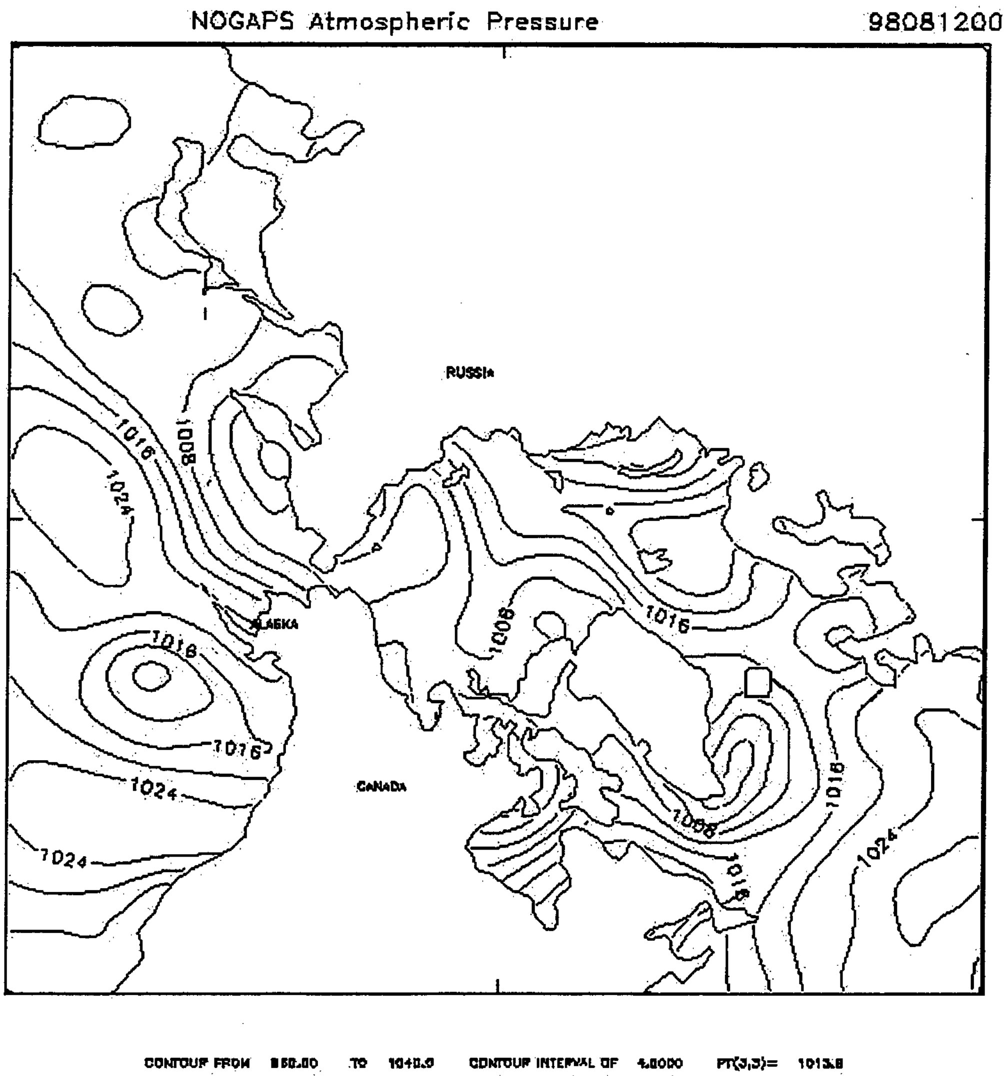

Figure 27. Atmospheric surface pressure chart for the first summer noise event (12 Aug 98). Note the presence of a weak low pressure trough extending from the Kamchatka Peninsula into the SHEBA region creating moderate (6-8 m/s) wind speeds and inducing a wind direction change.

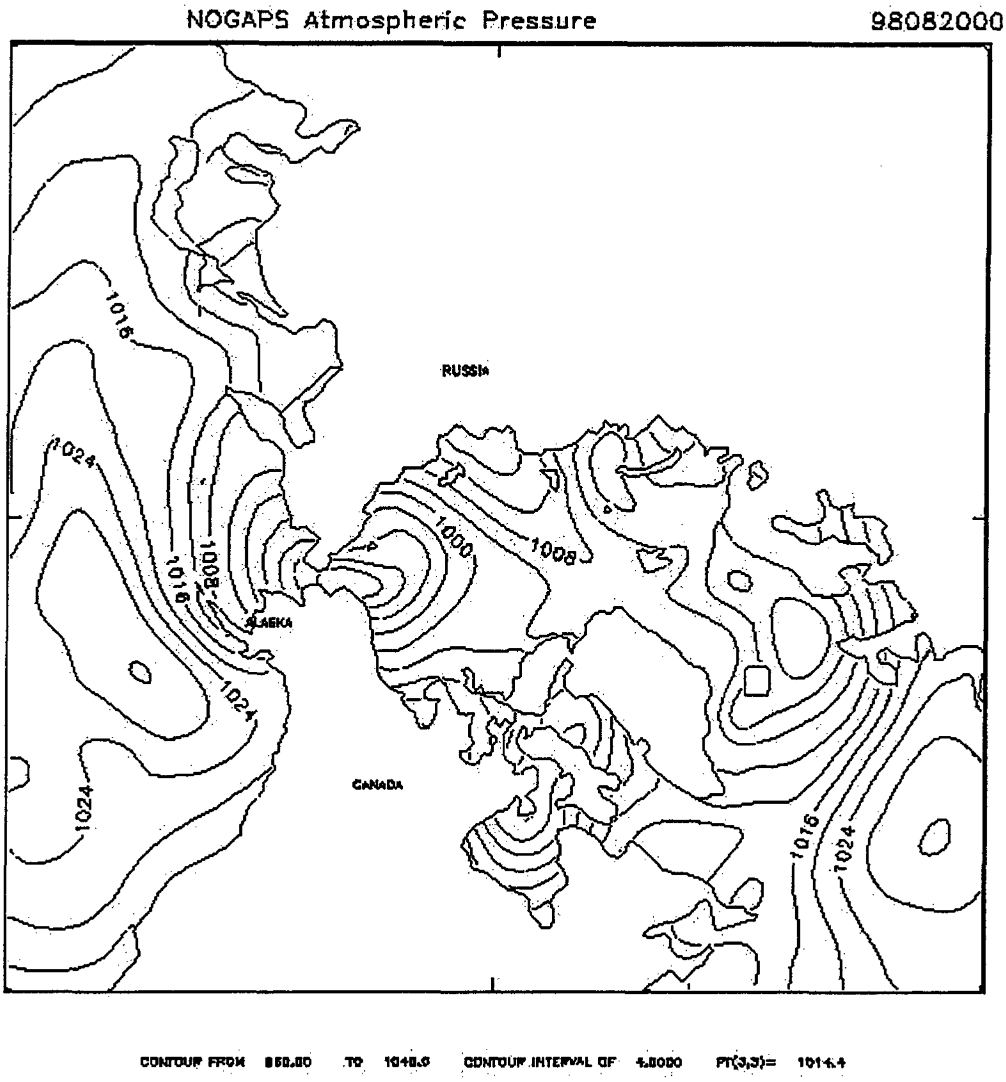

Figure 28. Atmospheric surface pressure chart for the second noise event (20 Aug 98). Note that a strong trough of low pressure extends from the Bering Strait into the SHEBA region causing another wind direction change along with high southerly winds (17 m/s) that rapidly moved the ice (speeds of 30 cm/s) in the SHEBA area.

like motion of the ice drift during this time (Figure 29) while the increase in wind speed lead to ice drift speeds of 15 cm/s.

The high noise event of 19 August (597) was accompanied by an even deeper and more developed low pressure trough that not only induced a southerly to northerly wind shift from 20-26 August (600-606), but produced wind speeds of up to 17 m/s and ice drift speeds of 30 cm/s on 19 and 20 August (597 and 598). The sustained northerly winds resulted in a more linear ice drift than the 12 August (590) event.

An examination of the ice drift track revealed a strong correlation between rapid changes in the prevailing direction of the drift track with peak ambient noise levels. Two distinct course changes in each of the three ice drift tracks are annotated on Figure 29 with arrows. These two course changes occurred on 12 August (590) and 20-21 August (598-599), which correspond to peak noise levels well above the 95th percentile. This strongly suggests that extreme changes in the direction of the ice drift resulted in the convergence of the floes and subsequent high speed, high energy, ice-ice collisions.

5. Summary

The summer event analysis demonstrated that the PIPS energy dissipation and RGPS deformation products are not applicable for summer conditions (more open water, lower ice concentration). However, the summer noise record does show an improved correlation with meteorological conditions as individual floes responded more distinctly to changes in wind speed and direction. Therefore, high energy, ice-

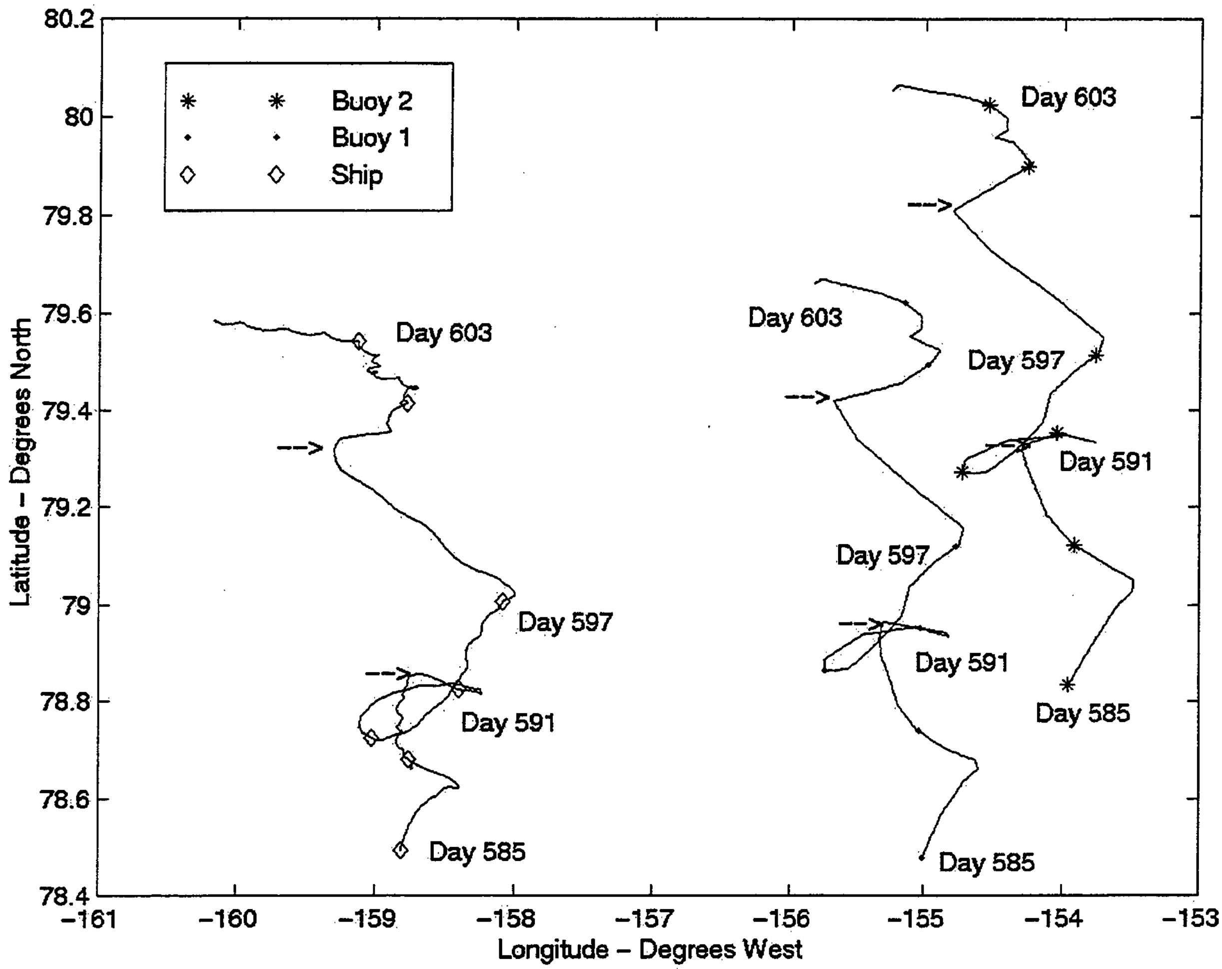

Figure 29. Drift track during the summer noise events. The arrows indicate a rapid change of ice drift direction and correspond to periods of extremely high noise levels.

ice collisions that resulted from changes in the wind speed and/or direction seemed to have been the dominant noise source during the summer.

E. SUMMARY OF SYNOPTIC EVENT ANALYSIS

The synoptic event analysis demonstrated a distinct seasonal difference in the noise field during the SHEBA experiment. During the winter, the highest levels of ambient noise were recorded during periods of convoluted, eddy-like motion, which caused convergence and subsequent development of pressure ridges in the continuous ice around the buoys. However, distant noise sources across the Arctic basin cannot be neglected as they were determined to have an appreciable effect on the noise record. As expected, noise levels received at the buoys during periods of distant ice deformation were lower than those received during local events due to increased transmission loss over the longer propagation distances. The main source of high level ambient noise during the winter was the forcing and deformation of the local region of the contiguous icepack, evident in the RGPS and PIPS energy dissipation plots.

During the summer, changing ice conditions caused the noise field to respond differently than the winter. Due to the increase of open water during the summer, PIPS energy dissipation and RGPS deformation were not applicable indicators of the ambient noise level. However, ambient noise levels were highly correlated with the intensity of meteorological forcing on the ice. Due to the fractured nature of the ice, high wind conditions produced high-energy, ice-ice collisions that produced periodic high noise levels. Large and rapid changes in the ice drift direction resulted in strong convergence of the icepack and also increased the likelihood of ice-ice collisions. Clearly, the energetic collisions of individual ice floes, rather than the fracturing and ridge building of the contiguous icepack during the winter, was the main source of high ambient noise levels during the summer.

Overall, the winter ambient noise field is a product of the nature of the contiguous icepack. Constant local and distant noise sources produce a rather high median noise level (approximately 60 dB), which deviates by as much as 20 dB during short-lived extreme loud or moderately quiet events. The summer noise record is characterized by long periods of low ambient noise (approximately 55 dB), when the individual floes are moving together, punctuated by brief periods of extremely high noise levels (as much as 30 dB greater than the median) when a storm causes the ice floes to collide.

THIS PAGE INTENTIONALLY LEFT BLANK

V. CONCLUSIONS AND RECOMMENDATIONS

A. CONCLUSIONS

The ambient noise data recorded by two free-drifting buoys during the 1997-98 SHEBA experiment presented a unique opportunity to gauge the noise field of the Arctic Ocean in a unique and changing environment. Ice concentration in the Arctic has continued to decrease over the past decade (Rothrock et al., 1999 and Morison et al., 1998), especially during the summer months, as evidenced by consecutive record low ice concentrations in September of 1997 and 1998 (Maslanik, 1999). At the same time, a long-term oscillation of atmospheric pressure in the region has affected meteorological conditions that drive ice motion (see Figure 1). Effects such as these will become increasingly important as efforts are made to model ambient noise in the Arctic.

Two tools to conceptualize the Arctic noise field were employed during the SHEBA experiment: the use of RADARSAT with RGPS and the PIPS computation of energy dissipation rate. By comparing the output from these two systems with the ambient noise record, their effectiveness and usefulness as input to an Arctic ambient noise model could be determined. Several notable events in the winter and summer noise record were examined utilizing RGPS and PIPS.

During the SHEBA experiment, the two ambient noise buoys were inserted on ice floes in the Beaufort Sea approximately 450 km north of Alaska. The placement pattern of the two buoys formed an isosceles triangle relative to the main SHEBA ice camp with one buoy deployed 55 km to the north and the other 70 km to the east of the SHEBA site. The buoys initially drifted in a westerly direction, concurrent with the southern sector of the anticyclonic Beaufort Gyre, before turning north for the second half of the experiment. Much of the late winter and early spring noise data were lost due to malfunctions within the hydrophone recording system. The buoys provided hourly measurements of ambient noise in 19 frequency bands of which 14, centered between 50 Hz and 1000 Hz, were utilized for this study. Meteorological data were recorded near the main SHEBA site.

The two buoys exhibited similar median spectra for all frequencies. When examined on a seasonal basis, summer low frequency (< 200 Hz) noise levels were much closer to winter noise levels than past studies. This was mainly due to the low number of storms during the winter of 1997-98, which resulted in lower winter median noise levels. The standard deviation increased with frequency, a characteristic associated with the high transmission loss of high frequency noise energy. This results in high frequency noise levels reflecting mainly local noise sources, which results in less consistency than low frequency noise levels, which have a larger number of potential noise sources (due to less transmission loss) and therefore more constant incoming noise energy.

When compared with previous ambient noise studies in the Beaufort Sea, the SHEBA noise data was consistent with the concept that noise levels decrease during years when cyclonic atmospheric circulation dominates the western Arctic. Divergence of the ice cover and reduced pressure ridge activity are the resultant products of this increase in cyclonic activity. This was most evident in the summer data, as 50 Hz noise levels were 7-10 dB less than those recorded during years when anti-cyclonic atmospheric circulation dominated the region. At high frequencies, the summer noise levels were comparable as both atmospheric patterns lead to reduced ice concentration and the occurrence of high-energy, ice-ice collisions.

The temporal coherency (as determined by the e-folding time) of 13-15 hours appears typical for observations made mid-way between the compact, high Arctic polar pack (e-folding times twice as large) and the fragmented nature of the marginal ice zone (e-folding times of 3-8 hours). The e-folding times generally decreased with frequency during the winter, similar to past studies, but increased with frequency during the summer. Open ice conditions in the summer lead to long periods of consistently low ambient noise, which was reflected by the high temporal coherency at high frequencies.

Cross correlation analysis indicated a strong association of wind speed and wind stress to ambient noise. Locally measured wind stress (as opposed to that computed using the geostrophic wind) did not substantially improve the correlation with ambient noise. The correlations strongly suggested that the ice drift in this deep-water part of the Arctic is predominantly wind driven and not greatly influenced by tides or topographically driven currents.

The influence of wind forcing is further demonstrated by the partitioning of each buoy trajectory into four segments or legs, each corresponding to a significant, long-term direction of forcing. The examination in detail of each leg revealed that the ambient noise level appeared to be controlled by the seasonal change in ice concentration and the degree of non-linear, eddy-like motions and subsequent rapid heading changes of the ice drift. During Leg 1, the buoys drifted westward with the prevailing wind. Occasional reversals to the east or deviations to the south were accompanied by an abrupt increase (anywhere from 10-15 dB) in the noise level. Pressure ridge building was a major source of ambient noise during this time as the consolidated pack ice responded to stress caused by changes in the wind direction. During the summer (Legs 3,4,5), the overall ambient noise level decreased as the open ice conditions permitted free-drift of the individual floes, which reduced the build up of internal stress in the ice. Long periods of low ambient noise were interrupted by short-lived, high noise level events that were characterized by rapid changes in wind and ice drift direction that resulted in an increased number of high energy, ice-ice collisions. The linear drift of Leg 3 was representative of a strong summer storm that resulted in a long-term (11 days) period of high winds and a sustained period of relatively high levels of ambient noise.

Four synoptic events were analyzed in order to investigate the nature of the forcing under loud and quiet noise conditions during both summer and winter. The synoptic event analysis demonstrated a distinct seasonal difference in the noise field during the SHEBA experiment. During the winter, the highest levels of ambient noise were recorded when the local ice field underwent periods of convoluted, eddy-like motion. Forcing from distant storms also produced an appreciable effect on the noise record, especially at low frequencies. RGPS and PIPS correlated well with local noise events, while the PIPS energy dissipation rate was also effective in characterizing distant noise events. During the summer, PIPS energy dissipation and RGPS deformation were not effective indicators of ambient noise due to the more open nature of the icepack, which prevented any buildup of internal energy. The independent motion of individual ice floes resulted in very low levels of energy dissipation rate and as random deformation to the RGPS sensors. Meteorological parameters (wind speed and wind stress) better corroborated the presence of high ambient noise levels during the summer.

B. RECOMMENDATIONS

Based on the results presented in the study, the following recommendations are made for improvements in subsequent research.

- Meteorological instruments need to be co-located with ambient noise buoys and record data at the same time interval as the ambient noise data record.
- The position of the buoys should be reported more often than twice per day in order to better resolve the mesoscale responses of the ice drift.
- The RGPS field should include the entire Arctic basin as it was shown in this study that distant deformation and subsequent noise energy can contribute to the local noise field.
- In order to accurately determine the bearings from which ambient noise energy is received, horizontal and vertical arrays should be deployed. This would aid in determining the contribution of distant noise sources and provide for a comparison between locally generated and distant forcing of the ice cover.

THIS PAGE INTENTIONALLY LEFT BLANK

APPENDIX A

DATA STATISTICS

FREQUENCY (Hz)	RECORD LENGTH (DAYS)	RECORD LENGTH (DAYS)	MISSING OR BAD DATA (HOURS)	MISSING OR BAD DATA (PERCENT)
50	115	2740	225	8.2%
63	115	2740	225	8.2%
80	115	2740	223	8.1%
100	115	2740	223	8.1%
125	115	2740	224	8.2%
160	115	2740	227	8.3%
200	115	2740	224	8.2%
250	115	2740	223	8.1%
320	115	2740	223	8.1%
400	115	2740	223	8.1%
500	115	2740	223	8.1%
640	115	2740	223	8.1%
800	115	2740	223	8.1%
1000	115	2740	223	8.1%

FREQUENCY (Hz)	RECORD LENGTH (DAYS)	RECORD LENGTH (DAYS)	MISSING OR BAD DATA (HOURS)	MISSING OR BAD DATA (PERCENT)
50	54	1292	166	12.8%
63	54	1292	168	12.9%
80	54	1292	165	12.8%
100	54	1292	169	13.0%
125	54	1292	168	12.9%
160	54	1292	167	12.9%
200	54	1292	166	12.8%
250	54	1292	165	12.8%
320	54	1292	165	12.8%
400	54	1292	165	12.8%
500	54	1292	165	12.8%
640	54	1292	165	12.8%
800	54	1292	166	12.8%
1000	54	1292	165	12.8%

XV. Noise data summary for Buoy 1 (top) and Buoy 2 (bottom) during Leg 1.

FREQUENCY (Hz)	RECORD LENGTH (DAYS)	RECORD LENGTH (DAYS)	MISSING OR BAD DATA (HOURS)	MISSING OR BAD DATA (PERCENT)
50	26	632	18	2.8%
63	26	632	20	3.1%
80	26	632	17	2.7%
100	26	632	18	2.8%
125	26	632	17	2.7%
160	26	632	16	2.5%
200	26	632	17	2.7%
250	26	632	16	2.5%
320	26	632	18	2.8%
400	26	632	16	2.5%
500	26	632	16	2.5%
640	26	632	17	2.7%
800	26	632	16	2.5%
1000	26	632	16	2.5%

FREQUENCY (Hz)	RECORD LENGTH (DAYS)	RECORD LENGTH (DAYS)	MISSING OR BAD DATA (HOURS)	MISSING OR BAD DATA (PERCENT)
50	26	632	54	8.5%
63	26	632	58	9.1%
80	26	632	52	8.2%
100	26	632	50	7.9%
125	26	632	51	8.1%
160	26	632	49	7.7%
200	26	632	49	7.7%
250	26	632	51	8.1%
320	26	632	49	7.7%
400	26	632	50	7.9%
500	26	632	51	8.1%
640	26	632	49	7.7%
800	26	632	50	7.9%
1000	26	632	49	7.7%

XVI. Noise data summary for Buoy 1 (top) and Buoy 2 (bottom) during Leg 2.

FREQUENCY (Hz)	RECORD LENGTH (DAYS)	RECORD LENGTH (DAYS)	MISSING OR BAD DATA (HOURS)	MISSING OR BAD DATA (PERCENT)
50	11	260	8	3.0%
63	11	260	9	3.5%
80	11	260	10	3.9%
100	11	260	9	3.5%
125	11	260	9	3.5%
160	11	260	7	2.7%
200	11	260	7	2.7%
250	11	260	8	3.0%
320	11	260	6	2.3%
400	11	260	7	2.7%
500	11	260	6	2.3%
640	11	260	7	2.7%
800	11	260	7	2.7%
1000	11	260	6	2.3%

FREQUENCY (Hz)	RECORD LENGTH (DAYS)	RECORD LENGTH (DAYS)	MISSING OR BAD DATA (HOURS)	MISSING OR BAD DATA (PERCENT)
50	11	260	24	9.2%
63	11	260	25	9.6%
80	11	260	25	9.6%
100	11	260	24	9.2%
125	11	260	26	10%
160	11	260	24	9.2%
200	11	260	25	9.6%
250	11	260	25	9.6%
320	11	260	23	8.8%
400	11	260	22	8.5%
500	11	260	23	8.8%
640	11	260	23	8.8%
800	11	260	22	8.5%
1000	11	260	23	8.8%

XVII. Noise data summary for Buoy 1 (top) and Buoy 2 (bottom) during Leg 3.

FREQUENCY (Hz)	RECORD LENGTH (DAYS)	RECORD LENGTH (DAYS)	MISSING OR BAD DATA (HOURS)	MISSING OR BAD DATA (PERCENT)
50	37	884	34	3.8%
63	37	884	35	4.0%
80	37	884	34	3.8%
100	37	884	34	3.8%
125	37	884	34	3.8%
160	37	884	36	4.1%
200	37	884	34	3.8%
250	37	884	35	4.0%
320	37	884	33	3.7%
400	37	884	34	3.8%
500	37	884	33	3.7%
640	37	884	32	3.6%
800	37	884	33	3.7%
1000	37	884	32	3.6%

FREQUENCY (Hz)	RECORD LENGTH (DAYS)	RECORD LENGTH (DAYS)	MISSING OR BAD DATA (HOURS)	MISSING OR BAD DATA (PERCENT)
50	37	884	57	6.4%
63	37	884	57	6.4%
80	37	884	57	6.4%
100	37	884	58	6.6%
125	37	884	57	6.4%
160	37	884	59	6.7%
200	37	884	57	6.4%
250	37	884	58	6.6%
320	37	884	57	6.4%
400	37	884	58	6.6%
500	37	884	58	6.6%
640	37	884	57	6.4%
800	37	884	58	6.6%
1000	37	884	57	6.4%

XVIII. Noise data summary Buoy 1 (top) and Buoy 2 (bottom) during Leg 4.

LEG NUMBER	Gap Length (Hours)	# of Occurrences
ONE	1	38
	2	18
	3	10
	4	2
	5	3
	6	4
	7	1
	8	3
	9	1
	10	2
	11	2
	13	2
	27	1
	28	1
	37	1
	44	1
TWO	1	12
	2	9
	3	8
	4	1
	5	1
	7	1
	8	1
	9	1
	11	1
	12	1
THREE	1	5
	2	2
	3	1
	4	1
	5	1
	8	1
	11	2
	16	1
FOUR	1	30
	2	9
	3	8
	4	2
	5	4
	6	3
	8	2
	9	1
	12	1
	13	1
	14	1
	15	1
	16	1

XIX. Lengths (in hours) of gaps in the meteorological data record.

	Frequency (Hz)	Mean (dB // 1μPA^2/Hz)	Median (dB // 1μPA^2/Hz)	Standard Deviation (dB)
Buoy 1	50	59.25	59.26	3.64
	63	60.83	60.71	3.89
	80	60.99	60.80	4.29
Winter 1997/1998	100	61.18	61.00	4.60
	125	60.94	60.70	4.95
	160	60.04	59.90	5.39

	Frequency (Hz)	Mean (dB // 1μPA^2/Hz)	Median (dB // 1μPA^2/Hz)	Standard Deviation (dB)
	50	60.24	60.00	3.08
Buoy 2	63	61.71	61.40	3.26
	80	61.85	61.62	3.57
	100	61.95	61.74	3.86
Winter 1997/1998	125	61.43	61.23	4.12
	160	60.49	60.62	4.49
	200	59.19	59.19	5.01
	250	57.77	57.80	5.56
	320	56.32	56.36	5.90
	400	54.48	54.40	6.14
	500	52.85	52.70	6.26
	640	51.30	51.29	6.29
	800	49.62	49.80	6.33
	1000	48.14	47.90	6.47

XX. Summary noise data statistics for Buoy 1 (top) and Buoy 2 (bottom) during winter 1997/1998.

	Frequency (Hz)	Mean (dB // $1\mu PA^2/Hz$)	Median (dB // $1\mu PA^2/Hz$)	Standard Deviation (dB)
Buoy 1 Summer 1998	50	57.56	57.00	5.20
	63	58.68	57.70	5.59
	80	57.70	56.60	5.97
	100	56.77	56.00	5.86
	125	55.72	55.10	5.91
	160	54.12	53.70	5.88
	200	52.15	51.70	5.85
	250	50.53	50.30	5.87
	320	48.82	48.50	5.87
	400	46.80	46.40	5.85
	500	46.11	45.70	5.99
	640	44.49	44.00	5.85
	800	43.73	43.10	5.61
	1000	42.01	41.40	5.45

	Frequency (Hz)	Mean (dB // $1\mu PA^2/Hz$)	Median (dB // $1\mu PA^2/Hz$)	Standard Deviation (dB)
Buoy 2 Summer 1998	50	58.69	57.80	5.59
	63	59.57	58.40	5.84
	80	58.77	57.70	6.11
	100	58.17	57.40	6.06
	125	57.12	56.50	6.17
	160	55.79	55.30	6.28
	200	54.35	53.90	6.34
	250	52.88	52.60	6.48
	320	51.30	50.90	6.69
	400	49.68	49.35	6.93
	500	48.30	47.95	6.91
	640	46.97	46.60	6.52
	800	45.56	45.20	6.40
	1000	44.16	43.60	6.30

XXI. Summary noise data statistics for Buoy 1 (top) and Buoy 2 (bottom) during summer 1998.

LIST OF REFERENCES

Bannister, R.W., R.N. Denham and K.M. Guthrie, D.G. Browning, and A.J. Perrone, "Variability of Low-Frequency Ambient Sea Noise," *J. Acoust. Soc. Am.*, **65**,1156-1163 (1979).

Bourke, R.H., Naval Postgraduate School (Personal Communication, 2000).

Bourke, R.H., D. Feller and J.H. Wilson, "Ambient Noise Characteristics of the Nansen Basin," submitted to *J. Acoust. Soc. Am.* (1999).

Bourke, R.H. and A.R. Parsons, "Ambient Noise Characteristics of the Northwestern Barents Sea," *J. Acoust. Soc. Am.*, **94**(5), 2799-2808 (1993).

Bourke, R.H. and R.P. Garrett, "Sea Ice Thickness Distribution in the Arctic Ocean," *Cold Regions Sci. Tech.*, **13**, 259-280 (1987).

Buck, B.M. and J.H. Wilson, "Nearfield Noise Measurements from an Arctic Pressure Ridge," *J. Acoust. Soc. Am.,* **80**, 256-264 (1986).

Buck, B.M. and M.W. Clarke, "Relating Arctic Under-Ice Ambient Noise with Environmental Factors," (U) Tech. Rept. 114, Naval Oceanographic Office, Bay St. Louis, MS (1989) (confidential).

Dyer, I., "Speculations on the Origin of Low Frequency Arctic Ocean Noise," in *Sea Surface Sound, Natural Mechanisms of Surface Generated Noise in the Ocean,* edited by B.R. Kerman (Kluwer Academic Publishers, Netherlands, 1988), pp. 513-530.

Feller, D., "Environmental Forcing of Ambient Noise in the Nansen and Amundsen Basin of the Arctic Ocean," Master's Thesis, Naval Postgraduate School, Monterey, CA, (September 1994).

Guest, P., Naval Postgraduate School (Personal Communication, 2000).

Hibler III, W.D., "A Dynamic Thermodynamic Sea Ice Model," *J. Phys. Oceanogr.*, **9**, 815-846, (1979).

Kinsler, L.E., A.R. Frey, A.B. Coppens and J.V. Sanders, *Fundamentals of Acoustics*, 3rd edition (John Wiley and Sons, New York, NY, 1982), p. 249.

Kwok, R. Jet Propulsion Laboratory, Pasadena, CA (Personal Communication, 1999).

Kwok, R., "The RADARSAT Geophysical Processor System," Unpublished manuscript, Jet Propulsion Laboratory, Pasadena, CA (1997).

Lewis, J.K. and W.G. Denner, "Arctic Ocean Noise Generation due to Pack Ice Kinematics and Heat Fluxes," *J. Acoust. Soc. Am.*, **88**, 549-565 (1988).

Maslanik, J.A., M.C. Serreze and T. Agnew, "On the Record Reduction in Western Arctic Sea-Ice Cover in 1998," *Geophys. Res. Lett.*, **26** (13), 1905-1908.

McPhee, M.G., T.P. Stanton, J.H. Morison and D.G. Martinson, "Freshening of the Upper Ocean in the Central Arctic: Is Perennial Ice Disappearing?" *Geophys. Res. Lett.*, **25**, 1729-1732 (1998).

Morison, J., K. Aagaard and M. Steele, "Study of the Arctic Change Workshop Held November 10-12, 1997," *Polar Science Center Rept.* No. 8, Applied Physics Laboratory, Univ. Washington, Seattle, WA, (1998).

National Snow and Ice Data Center, SSM/I NASA Algorithm computed ice concentration during the SHEBA experiment. [http://www-nsidc.colorado.edu] (1998).

Nordman, M.Z., "An Analysis of Drifting Buoy Ambient Noise Data in the Beaufort Sea," Master's Thesis, Naval Postgraduate School, Monterey, CA, (December 1989).

Oard, V.T., "Characteristic Spectral Signatures of Arctic Noise Generating Mechanisms," Master's Thesis, Naval Postgraduate School, Monterey, CA, (June 1987).

Oceanographer of the Navy, "History and Practice of Naval Oceanography." [http://oceanographer.navy.mil] (2000).

Parsons, A.R., "Environmental Forcing of Ambient Noise in the Barents Sea," Master's Thesis, Naval Postgraduate School, Monterey, CA, (June 1992).

Perovich, D.K., E.L. Andreas, J.A. Curry, H. Eiken, C.W. Fairall, T.C. Grenfell, P.S. Guest, J. Intrieri, D. Kadko, R.W. Lindsay, M.G. McPhee, J. Morison, R.E. Moritz, C.A. Paulson, W.S. Pegau, P.O.G. Persson, R. Pinkel, J.A. Richter-Menge, T. Stanton, H. Stern, M. Sturm, W.B. Tucker III and T. Uttal, "Year on Ice Gives Climate Insights," *EOS*, **80**(41), 481-486, (1999).

Poffenberger, D.L., "Analysis of Arctic Ambient Noise Measured from Drifting Buoys in the Greenland Sea and Eurasian Basin," (U) Master's Thesis, Naval Postgraduate School, Monterey, CA, (December 1987). (confidential)

Polyakov, I.V., A. Proshutinsky and M.A. Johnson, "Seasonal Cycles in Two Regimes of Arctic Climate," *J. Geophys. Res.*, **104**(C11) (1999).

Pritchard, R.S., "A Simulation of Nearshore Winter Ice Dynamics in the Beaufort Sea," in *Sea Ice Processes and Models*, edited by R.S. Pritchard (University of Washington Press, Seattle, WA, 1980), pp.49-61.

Proshutinsky, A. and M.A. Johnson, "Two Circulation Regimes of the Wind-Driven Arctic Ocean," *J. Geophys. Res.*, **102**(C6), 12493-12514 (1997).

Proshutinsky, A., I.V. Polyakov and M.A. Johnson, "Climate States and Variability of Arctic Ice and Water dynamics 1946-1997," *Polar Research*, **18,** 1-8 (1999).

Rothrock, D.A., Y. Yu and G.A. Maykut, "Thinning of the Arctic Sea-Ice Cover," *J. Geophys. Res.*, **26**, 3469-3472, (1999).

Urick, R.J. *Principles of Underwater Sound*, 3rd Edition (McGraw-Hill Book Company, New York, NY, 1983).

THIS PAGE INTENTIONALLY LEFT BLANK

INITIAL DISTRIBUTION LIST

1.	Defense Technical Information Center Cameron Station Alexandria, VA	2
2.	Library, Code 52 Naval Postgraduate School Monterey, CA 92943-5000	2
3.	Chairman (Code OC/BF) Department of Oceanography Naval Postgraduate School Monterey, CA 92943-5000	1
4.	Prof. Robert H. Bourke (Code OC/BF) Department of Oceanography Naval Postgraduate School Monterey, CA 92943-5000	2
5.	Dr. James H. Wilson Neptune Sciences, Inc. 3834 Vista Azul San Clemente, CA 92674	1
6.	LT Ronald R. Shaw Jr. 1812 N. Bristol St. Tacoma, WA 98406	2
7.	Commander Naval Meteorology and Oceanography Command 1020 Bach Blvd. Stennis Space Center, MS 39529-5005	1
8.	Dr. Dennis Conlon (Code 322 (HL)) Office of Naval Research 800 N. Quincy St. Arlington, VA 22217-5660	1
9.	Dr. Ronald Kwok JPL MS 300-235 Pasadena, CA 91109	1

10. Dr. William Hibler, III 1
International Arctic Research Center
University of Alaska, Fairbanks
930 Koyukuk Dr.
P.O. Box 75735
Fairbanks, AK 99775-7335

11. Dr. Ruth Preller/Ms. Pam Posey 1
Naval Research Laboratory (Code 7322)
Stennis Space Center, MS 39529-5005

12. Dr. Peter Stein 1
Scientific Solutions, Inc.
99 Perimeter Rd.
Nashua, NH 03063

13. Dr. Robert S. Pritchard 1
Ice Casting, Inc.
1368 Lincoln Avenue, Suite 209
San Rafael, CA 94901-9899

14. Dr. Richard E. Mortiz 1
Polar Science Center
Applied Physics Laboratory
University of Washington
1013 N.E. 40th Street
Seattle, WA 98105-6698

14. Dr. Peter S. Guest (Code MR) 1
Department of Meteorology
Naval Postgraduate School
Monterey, CA 92943-5000